

Library Copy

R.A. 212388 R.O.1

UNCLASSIFIED

Copy
RM SL58H15

2183

NACA

CLASSIFICATION CHANGE

UNCLASSIFIED

Re: NACA AD 11-67, 15-11-71, 26-11-71
Classified by *DKM* 3/98 Date *26-11-71*

RESEARCH MEMORANDUM

for the

Bureau of Aeronautics, Department of the Navy

LOW-SPEED WIND-TUNNEL TESTS OF A 1/8-SCALE

MODEL OF THE BELL D-188A VTOL AIRPLANE

TED NO. NACA AD 3147

By Marion O. McKinney and Charles C. Smith, Jr.

Langley Aeronautical Laboratory
Langley Field, Va.

UNCLASSIFIED

CLASSIFICATION CHANGE

CLASSIFIED DOCUMENT

This material contains information affecting the National Defense of the United States within the meaning of the espionage laws, Title 18, U.S.C., Secs. 793 and 794, the transmission or revelation of which in any manner to an unauthorized person is prohibited by law.

LIBRARY COPY

AUG 25 1958

LANGLEY AERONAUTICAL LABORATORY
LIBRARY, NACA
LANGLEY FIELD, VIRGINIA

NATIONAL ADVISORY COMMITTEE
FOR AERONAUTICS

WASHINGTON

AD-3147

UNCLASSIFIED



NATIONAL ADVISORY COMMITTEE FOR AERONAUTICS
RESEARCH MEMORANDUM

for the
Bureau of Aeronautics, Department of the Navy

LOW-SPEED WIND-TUNNEL TESTS OF A 1/8-SCALE
MODEL OF THE BELL D-188A VTOL AIRPLANE*

TED NO. NACA AD 3147

By Marion O. McKinney and Charles C. Smith, Jr.

SUMMARY

An investigation has been conducted to determine the low-speed power-off stability and control characteristics of a 1/8-scale model of the Bell D-188A vertical-take-off-and-landing (VTOL) airplane. This airplane is a horizontal-attitude VTOL fighter with tilting engine nacelles at the tips of a low-aspect-ratio unswept wing. The results of the tests showed that the static stability and control characteristics of the model were generally satisfactory except that the model was directionally unstable at angles of attack above 13° and that the aileron effectiveness dropped off markedly as the angle of attack was increased from 0° to 16° . The tests also showed that the model could be made directionally stable at angles of attack up to 23° by means of rather extensive modification to the vertical tails.

INTRODUCTION

An investigation of the low-speed stability and control characteristics of the Bell D-188A VTOL airplane is being conducted by the Langley Free-Flight Tunnel Section with a 1/8-scale flying model, a sketch of which is shown in figure 1. Part of this program has been a determination of the static stability and control characteristics of the model by means of wind-tunnel force tests. The results of these force tests are presented in the present paper with only a limited analysis for the use of the armed services and contractors interested in this configuration.

*Title, Confidential.

UNCLASSIFIED

UNCLASSIFIED

CLASSIFICATION CHANGED

2-16-66
Bmd
2-8-66

The investigation consisted of tests to determine the longitudinal and lateral stability and control characteristics of the model in the original configuration and tests to determine the causes and possible cures for the directional instability and loss in aileron effectiveness at high angles of attack which had shown up in preliminary force and flight tests of the model.

SYMBOLS

The longitudinal forces and moments are referred to the stability axes and the lateral forces and moments are referred to the body axes. These axes are shown in figure 2 which shows the positive direction of forces, moments, and angles. The symbols used in the paper are defined as follows:

S	wing area, sq ft
b	wing span, ft
\bar{c}	wing mean aerodynamic chord, ft
V	airspeed, ft/sec
ρ	air density
q	dynamic pressure, $\frac{\rho V^2}{2}$
α	angle of attack, deg
β	angle of sideslip, deg
i_t	horizontal tail incidence, positive for trailing edge down, deg
i_n	wing-tip nacelle incidence, positive for nose-up deflection, deg
δ_{a_l}	deflection of left aileron, positive for trailing edge down, deg
δ_{a_r}	deflection of right aileron, positive for trailing edge down, deg
F_L	lift, lb

F_D'	drag, lb
F_Y	lateral force, lb
M_Y	pitching moment, ft-lb
M_X	rolling moment, ft-lb
M_Z	yawing moment, ft-lb
C_L	lift coefficient, $\frac{F_L}{qS}$
C_D'	drag coefficient, $\frac{F_D'}{qS}$
C_Y	lateral-force coefficient, $\frac{F_Y}{qS}$
C_m	pitching-moment coefficient, $\frac{M_Y}{qSc}$
C_l	rolling-moment coefficient, $\frac{M_X}{qSb}$
C_n	yawing-moment coefficient, $\frac{M_Z}{qSb}$
$C_{Y\beta}$	variation of lateral-force coefficient with angle of sideslip, $\frac{\partial C_Y}{\partial \beta}$, per deg
$C_{l\beta}$	variation of rolling-moment coefficient with angle of sideslip, $\frac{\partial C_l}{\partial \beta}$, per deg
$C_{n\beta}$	variation of yawing-moment coefficient with angle of sideslip, $\frac{\partial C_n}{\partial \beta}$, per deg

Model component designations:

F	fuselage
W	wing
N	nacelle
H ₀	horizontal tail with 0° dihedral
H ₁₅	horizontal tail with -15° dihedral
H ₃₀	horizontal tail with -30° dihedral
V _U	original upper vertical tail
V _{U1} , V _{U2} , V _{U3}	modified upper vertical tails (see fig. 3)
V _L	original lower vertical tail
V _{L1} , V _{L2} , V _{L3} , V _{L4}	modified lower vertical tails (see fig. 3)

APPARATUS AND TESTS

A three-view sketch of the model in the original configuration is shown in figure 1. The wing-tip engine nacelles tilt through approximately 90° to a vertical attitude for vertical take-off and landing. In order to increase the inlet area and permit the engines to attain the maximum possible air flow for hovering and low-speed flight the inlets of the nacelles of the airplane slide forward, as indicated by the inset sketch in figure 1, to open a large inlet around the nacelle. It is planned that the inlets be open at airspeeds less than about 200 knots. The existence of this feature was not known until part of the tests had already been completed; therefore, all the earlier tests were made with the inlet in the high-speed condition and all of the later tests were made with the inlet moved forward to represent the low-speed flight condition. The model was equipped to be powered by compressed air jets for the flight tests, but all of the force tests reported herein were made with power off.

Some of the force tests were made in the Langley free-flight tunnel and some were made in the Langley full-scale tunnel (where the flight tests are being made) depending on the availability of these facilities

at the time the tests were required. It is not expected that results obtained in these two facilities would be greatly different, but the tunnel in which the tests were run is given in the list of test conditions presented in table I since the difference in test facility may be responsible for some small discrepancies in the data. The tests were run at a Reynolds number of about 500,000. The force-test data were reduced to coefficient form on the basis of the following dimensions of an effective wing extending to the center of the nacelles:

$$b = 2.70 \text{ ft}$$

$$S = 3.03 \text{ sq ft}$$

$$\bar{c} = 1.21 \text{ ft}$$

The effective aspect ratio based on these dimensions is 2.42.

A complete list of the tests conducted is given in table I. The test program generally fell into two parts: (1) tests to determine the longitudinal and lateral stability and control characteristics of the model in the original configuration and (2) tests to determine the causes and possible cures for the directional instability encountered at angles of attack above 13° in preliminary force and flight tests of the model. The various modified tail configurations tested are shown in figure 3. Various modifications to the wing and lateral controls investigated in an attempt to improve the aileron effectiveness are shown in figure 4.

RESULTS AND DISCUSSION

Stability and Control of Original Configuration

Longitudinal.— The longitudinal characteristics of the model with the nacelles at 0° incidence and the inlets retracted are presented in figure 5, for angles of attack up to 90° , and the effectiveness of the horizontal tail as a pitch control is shown in figure 6. These data show that the model was longitudinally stable over most of the angle-of-attack range except between angles of attack of 24° to 28° where it was about neutrally stable. The break in the lift curve at angles of attack near 12° is evidently caused by the wing stall as indicated by the results of the tuft tests presented in figure 7. These data show that the wing stall was well advanced at an angle of attack of 8° and

that the wing was almost completely stalled at an angle of attack of 16° . The increase in lift with increase in angle of attack above 16° , which is shown in figures 5 and 6, can be attributed to the increase in lift on the relatively large fuselage of the model.

The effect of the nacelles is shown in figure 8 which presents a direct comparison of the model with the nacelles off and on and with inlets retracted and extended for the normal angle-of-attack range. These data show that the nacelles cause a considerable destabilizing effect, but there was very little effect of extending the inlets.

The longitudinal characteristics of the model with the nacelles tilted at various angles of incidence up to 90° are presented in figure 9. These tests were made with the inlet in the high-speed condition and therefore may not represent the characteristics of the airplane very closely.

Lateral.— The lateral stability characteristics of the airplane with the nacelles at 0° incidence and with the inlets retracted are shown in figures 10 and 11. The values of the lateral stability derivatives given in figure 11 were determined from the difference between values in figure 10 at 5° and -5° sideslip. The rolling moments were very erratic at angles of attack above 16° and the rolling-moment data in this range are not considered reliable. For this reason no values of $C_{l\beta}$ above 16° angle of attack are shown in figure 11.

These data of figures 10 and 11 show that the model in the original configuration with the nacelles at 0° incidence is directionally unstable at angles of attack above 12° . Static directional instability such as this is not necessarily an indication of a directional divergence or dynamic instability of an airplane in flight. A few preliminary flight tests of the model have shown that it does diverge directionally at an angle of attack of about 15° . This directional instability therefore became the subject of more extensive studies which are covered in a later section of this paper.

The effect of the nacelle incidence on the lateral stability characteristics is shown in figure 12. These tests were made with the inlet in the high-speed rather than the low-speed condition; therefore, the data may not represent the characteristics of the airplane exactly.

The aileron effectiveness, in terms of the moments and forces produced by 40° total aileron deflection or 45° spoiler deflection, is shown in figure 13. These data show that the aileron effectiveness of the original configuration dropped off markedly as the angle of attack was increased from 0° to 16° . This result, in general, ties in with the results of the tuft tests presented in figure 7 which show that the

wing stall begins at the tips at a very low angle of attack and moves in progressively over the ailerons as the angle of attack is increased. The use of a leading-edge flap, which was intended to relieve the stall, reduced the drop-off of aileron effectiveness with increase in angle of attack and resulted in approximately a 30-percent increase in effectiveness at 16° angle of attack. The inboard ailerons used either alone or in conjunction with the spoiler gave much smaller rolling moments than the original ailerons throughout the angle-of-attack range. The aileron effectiveness data are not presented at angles of attack above 16° because the rolling moments became so erratic at higher angles that the data were not considered reliable.

Study of Directional Stability

The first step in the study of the directional-stability problem of the airplane was to make breakdown tests to determine the effect of various airplane components on the directional stability. Since the variation of the yawing moment with angle of sideslip shown in figure 10 was fairly linear, the breakdown tests and tests of various modified configurations were run only at 5° and -5° sideslip and the lateral stability derivatives determined from the difference in forces and moments at these two angles. The results of these tests are presented in figure 14. The data of figure 14 show that the effectiveness of the upper vertical tail drops off rapidly as the angle of attack increases up to about 16° or 20° . The effectiveness of the lower vertical tail is maintained over the angle-of-attack range for configurations with the wing on.

Since the lower vertical tail maintained its effectiveness over the angle-of-attack range (for the complete model) it seemed desirable to get as much directional stability as possible from tails below the fuselage. The contributions of various modified lower vertical tails are shown in figure 15. These data show that all of the modified tails except that with a simple increase in chord V_{11} increased the directional stability, but none of these tails alone made the model stable.

The effect of various modified upper vertical-tail configurations is shown in figure 16. These data show that all three of the enlarged tails V_{U1} , V_{U2} , and V_{U3} which were taller than the original tail had some effectiveness in the high angle-of-attack range where the original upper vertical tail was completely ineffective. This indicates that only the upper part of these tails are effective in the high angle-of-attack range and that any improvement in directional stability that is to be gained from modifying the upper vertical tail must be gained by increasing the height of the tail.

The possibility of increasing the directional stability by use of a greater negative dihedral of the horizontal tail is shown in figure 17. Tests were made with the tail dihedral increased from -15° to -30° for the case of vertical tails removed and for the case of several lower vertical tails to show any possible adverse effect of the horizontal tail dihedral on the effectiveness of the lower vertical tail. Analysis of the data of figures 17(a) and 15(b) show that the effectiveness of the lower vertical tail was reduced by changing the horizontal tail dihedral to -30° , but that the stability of the model with any given lower vertical tail was slightly greater with -30° tail dihedral than -15° dihedral.

The effect of strakes on the front of the fuselage is shown in figures 18 and 19. The data of figure 18(a) were obtained in a series of development tests to devise an effective strake configuration at an angle of attack of 20° where the directional stability of the model without strakes was unsatisfactory. The configuration which seemed most promising in these tests was then tested throughout the angle-of-attack range. This configuration and its directional stability characteristics are shown in figure 18(b). These data show that strakes provided only a slight improvement in the directional stability of the model. This result was disappointing in view of the fact that strakes have been very effective on some models in altering the sidewash from the fuselage nose and thereby increasing the directional stability. The data of figure 19 show that the strakes have practically no effect on the longitudinal characteristics of the model.

The data presented in figure 20 were obtained in order to check the combined effect of adding various modified tail components rather than rely on adding increments from tests of the separate components. These data show that the directional stability of the model was improved, but that the model was still unstable at high angles of attack with only the large upper vertical tail V_{U3} added. The data also show that the model was directionally stable at angles of attack up to 23° if the twin lower vertical tails V_{L4} and -30° dihedral of the horizontal tail were used in conjunction with the large upper vertical tail V_{U3} .

After the rest of the test program had been completed and the data analyzed, the manufacturer requested additional tests with the modified vertical-tail arrangement shown in figure 3(i). The results of these tests are presented in figure 21. These data show that the directional stability of the model was improved by this modification, but that this modification does not provide as much improvement at the higher angles of attack as either of the two configurations covered by figure 20.

CONCLUDING REMARKS

The results of the low-speed power-off wind-tunnel tests of a 1/8-scale model of the Bell D-188A VTOL airplane have indicated that the low-speed static stability and control characteristics of the model were generally satisfactory except that the model was directionally unstable at angles of attack above 13° and that the aileron effectiveness dropped off markedly as the angle of attack was increased from 0° to 16° . The tests also showed that the model could be made directionally stable at angles of attack up to 23° by means of rather extensive modifications to the vertical tails.

Langley Aeronautical Laboratory,
National Advisory Committee for Aeronautics,
Langley Field, Va., August 1, 1958.

TABLE I.- TEST PROGRAM

Tests	Test facility (a)	Figure
Longitudinal stability and control characteristics of original configuration	FFT	5, 6, and 8
Effect of nacelle incidence on longitudinal stability	FFT	9
Lateral stability of original configuration	FFT	10 and 11
Effect of nacelle incidence on lateral stability	FFT	12
Aileron effectiveness of original and modified ailerons	FFT	13
Effect of model components on lateral stability	FST	14
Effect of vertical tail modifications on lateral stability	FST	15 and 16
Effect of horizontal tail dihedral on lateral stability	FST	17
Effect of strakes on lateral and longitudinal stability	FFT	18 and 19
Effect of various combinations of modified vertical tails on lateral stability	FFT	20 and 21

^aFFT refers to the Langley free-flight tunnel, and FST refers to the Langley full-scale tunnel.

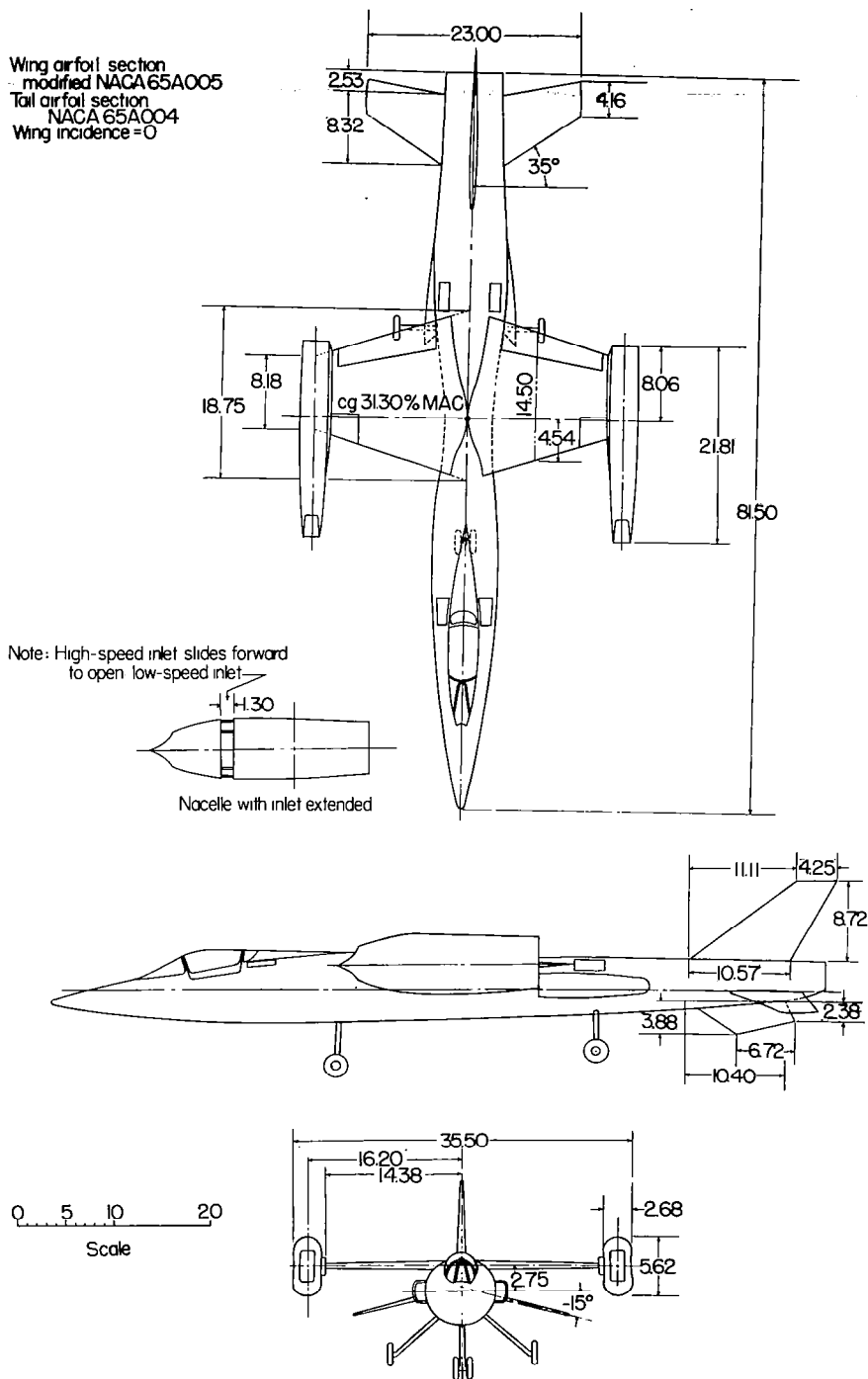


Figure 1.- Sketch of model in original configuration. All dimensions are in inches.

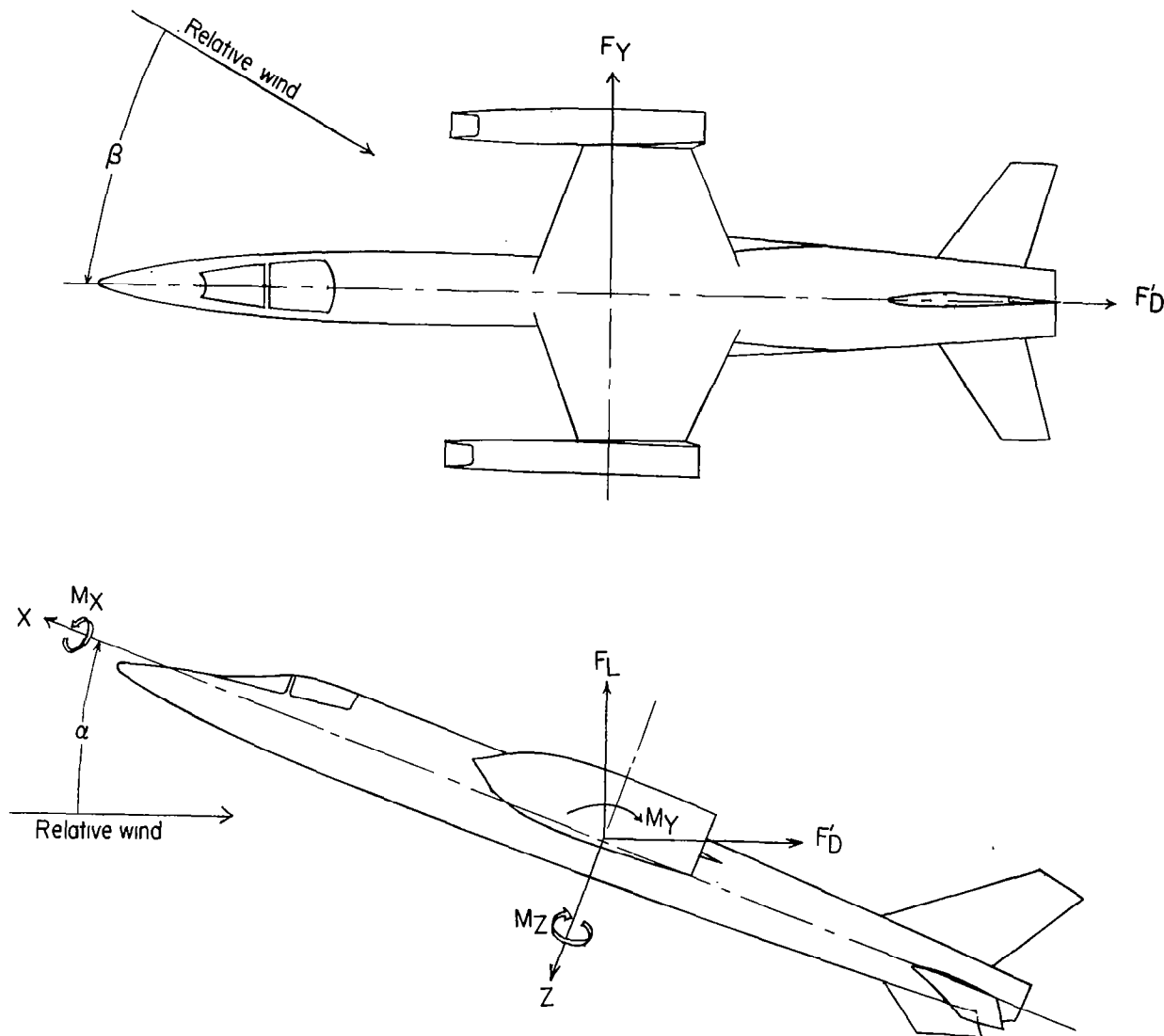


Figure 2.- Sketch of axes showing positive direction of forces, moments, and angles.

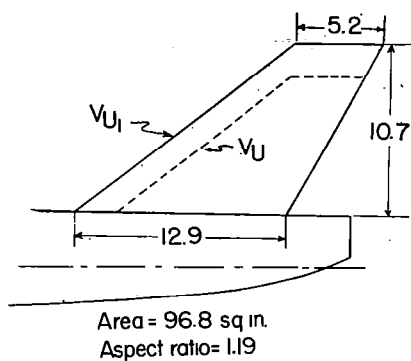
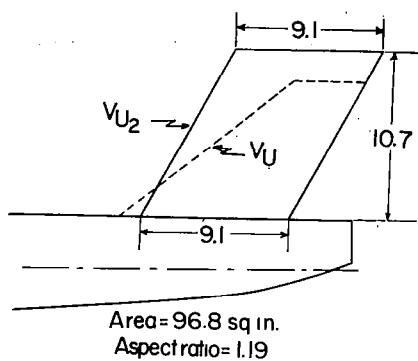
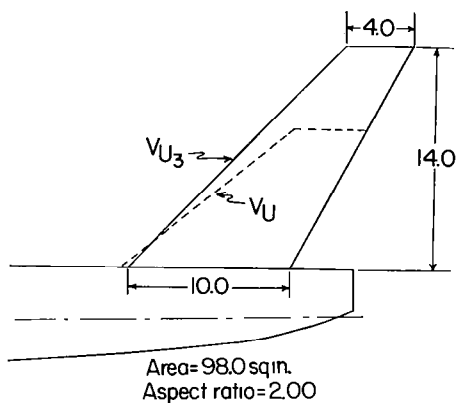
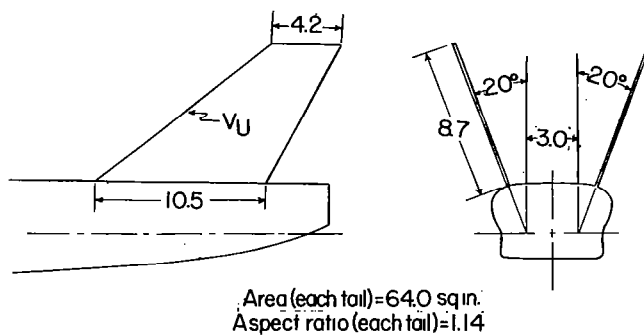
(a) V_{U1} .(b) V_{U2} .(c) V_{U3} .(d) Twin V_U .

Figure 3.- Modified vertical tails. All dimensions are in inches.

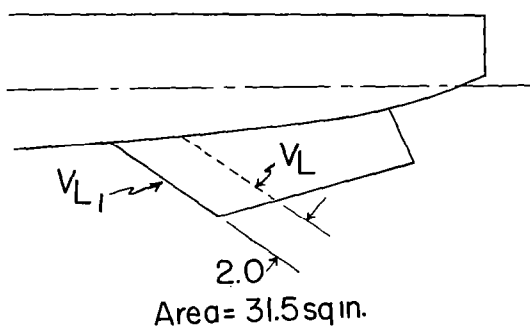
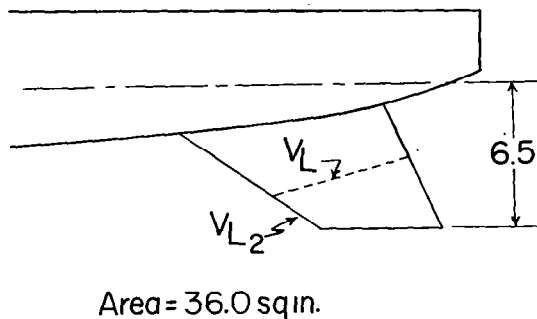
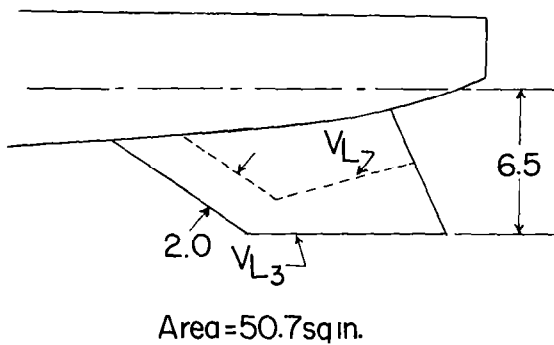
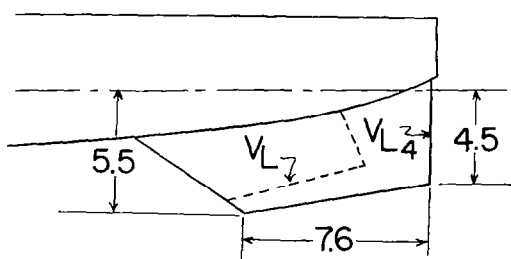
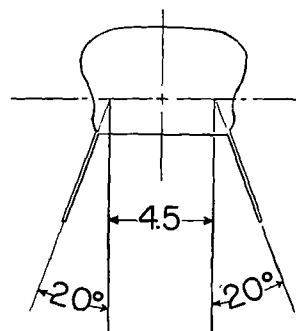
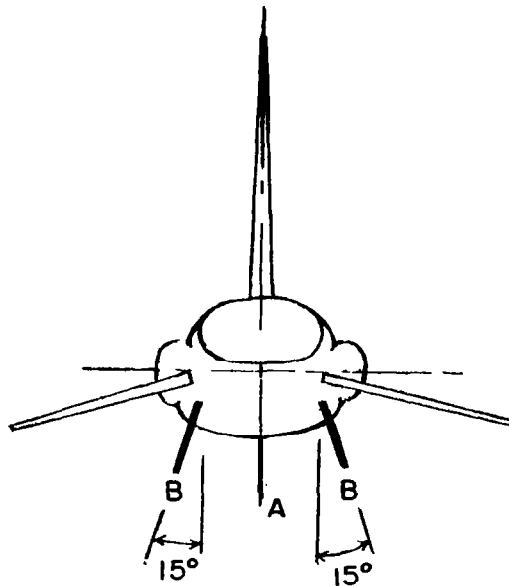
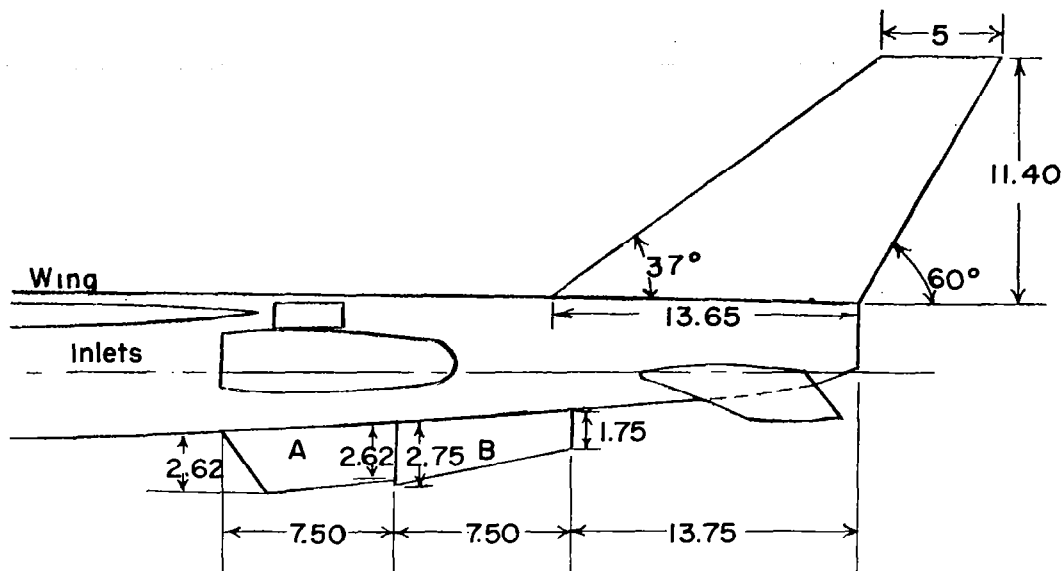
(e) V_{L1} .(f) V_{L2} .(g) V_{L3} .(h) Twin V_{L4} .

Figure 3.- Continued.



(i) Vertical-tail arrangement suggested by manufacturer.

Figure 3.- Concluded.

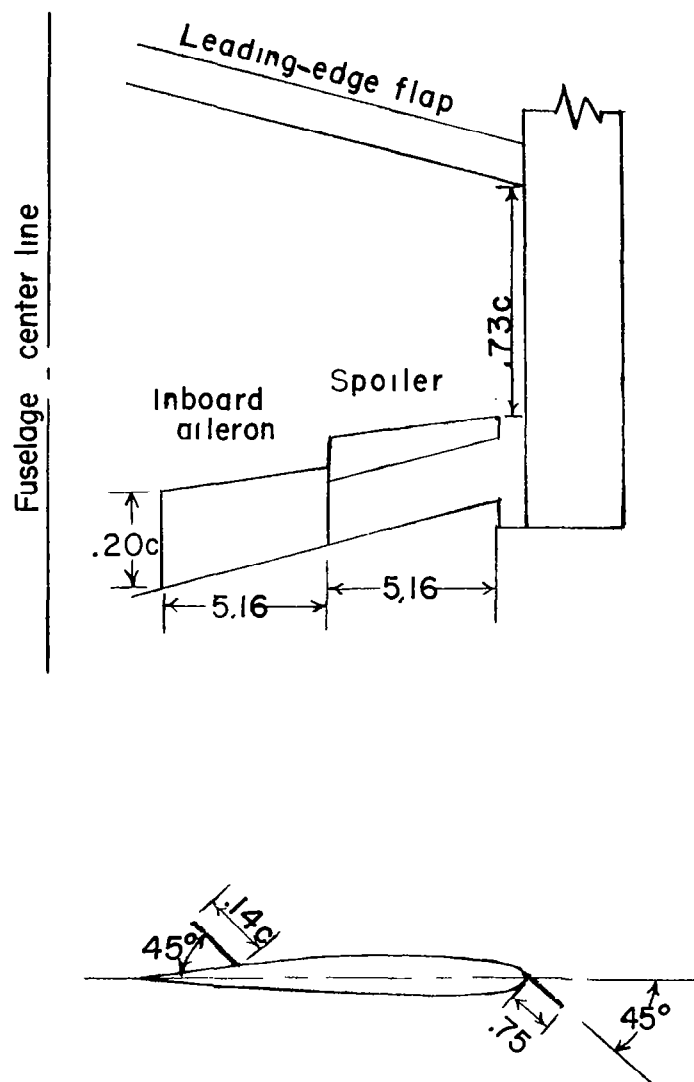


Figure 4.- Modified ailerons, spoilers, and leading-edge flap. All dimensions are in inches.

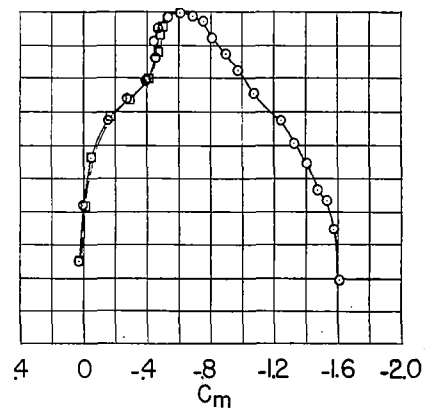
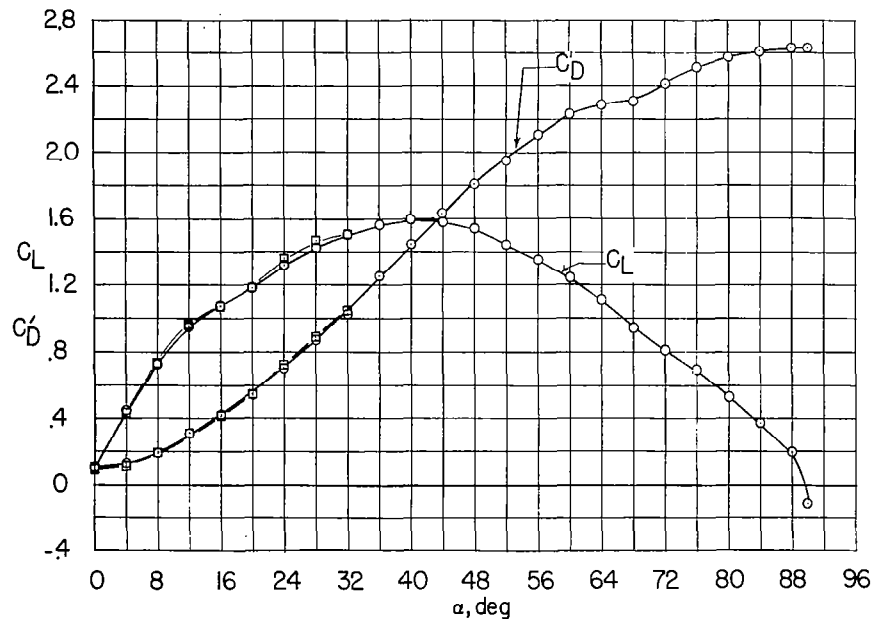
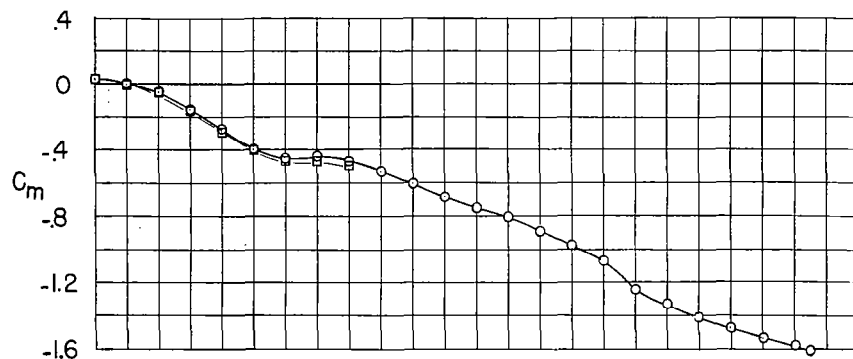


Figure 5.- Longitudinal stability characteristics for complete model configuration FWNH₁₅V_UV_L with nacelle inlets retracted. $i_n = 0^\circ$; $i_t = 0^\circ$.

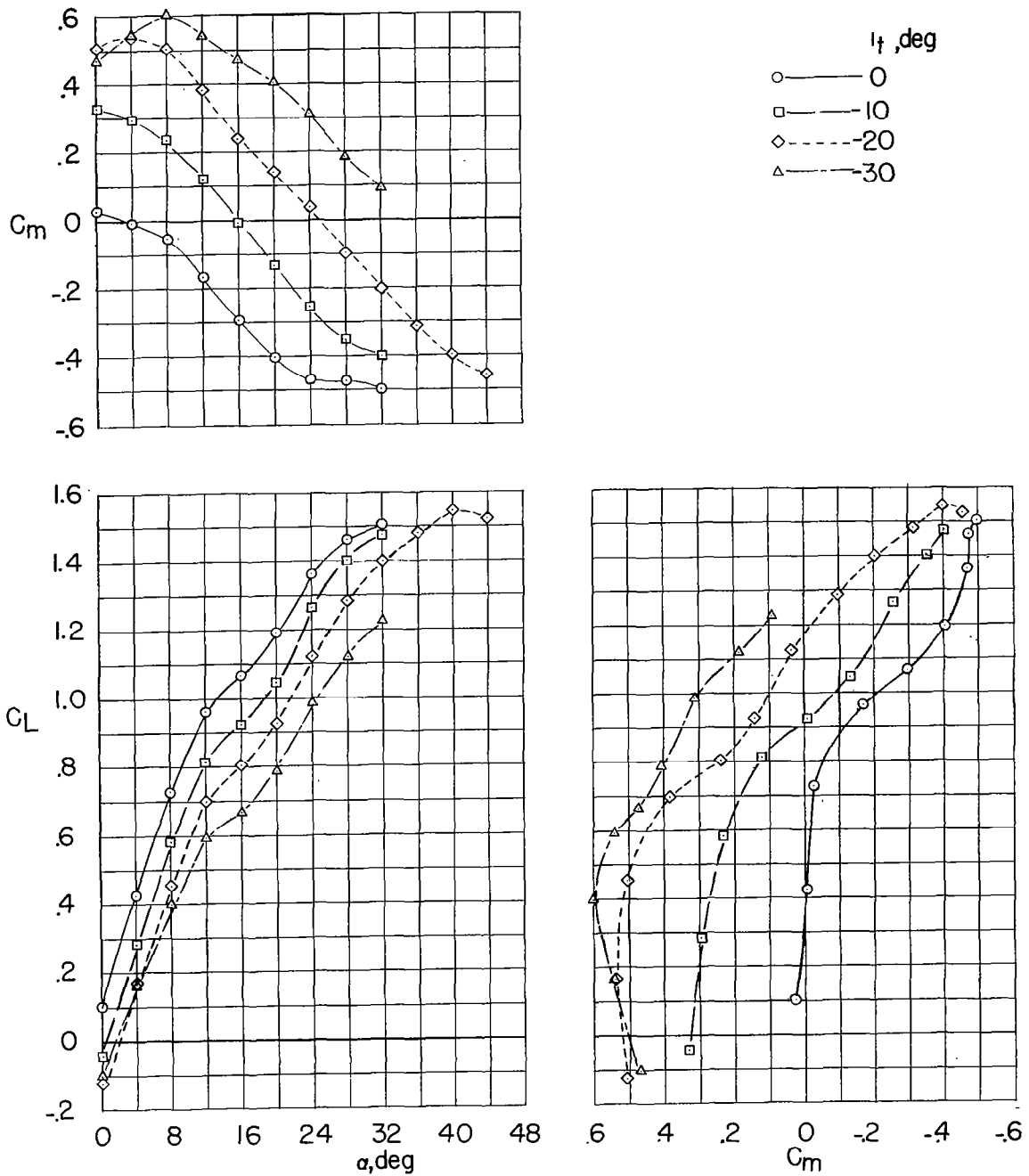


Figure 6.- Elevator effectiveness. Configuration FWNH₁₅V_UV_L with nacelle inlets retracted. $i_n = 0^\circ$.

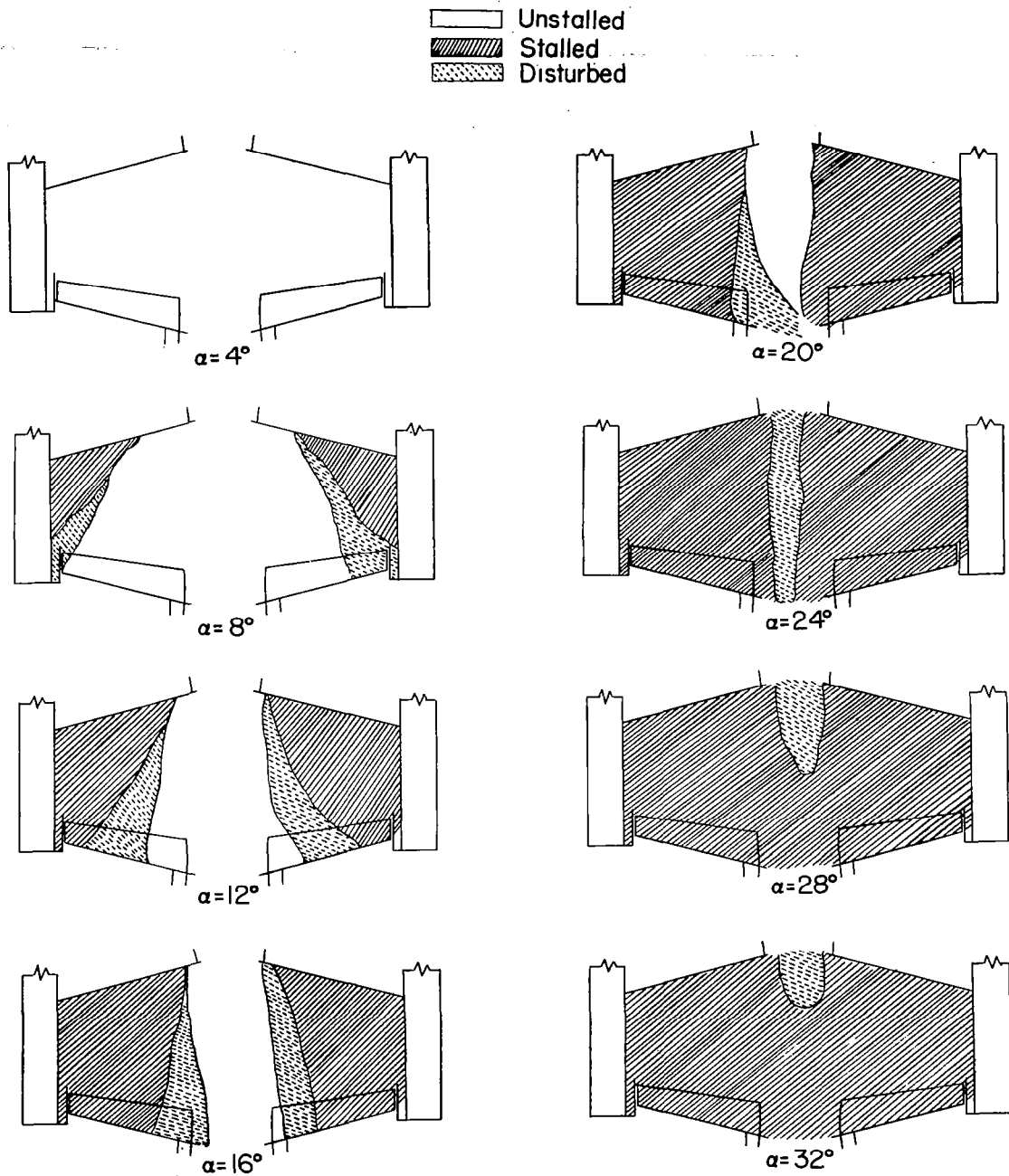


Figure 7.- Stall progression on upper surface of wing.

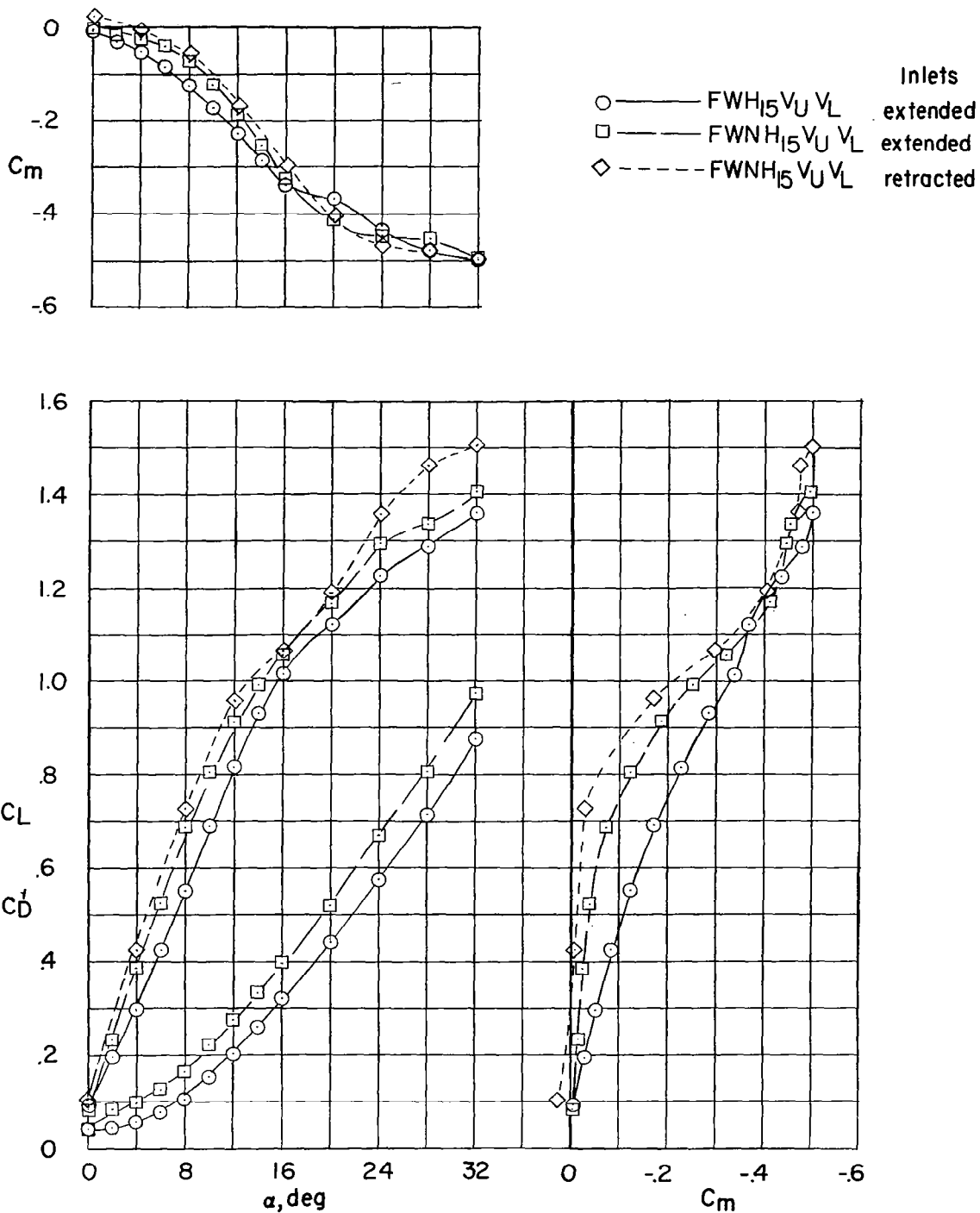


Figure 8.- Effect of nacelles on the longitudinal stability characteristics. $i_n = 0^\circ$.

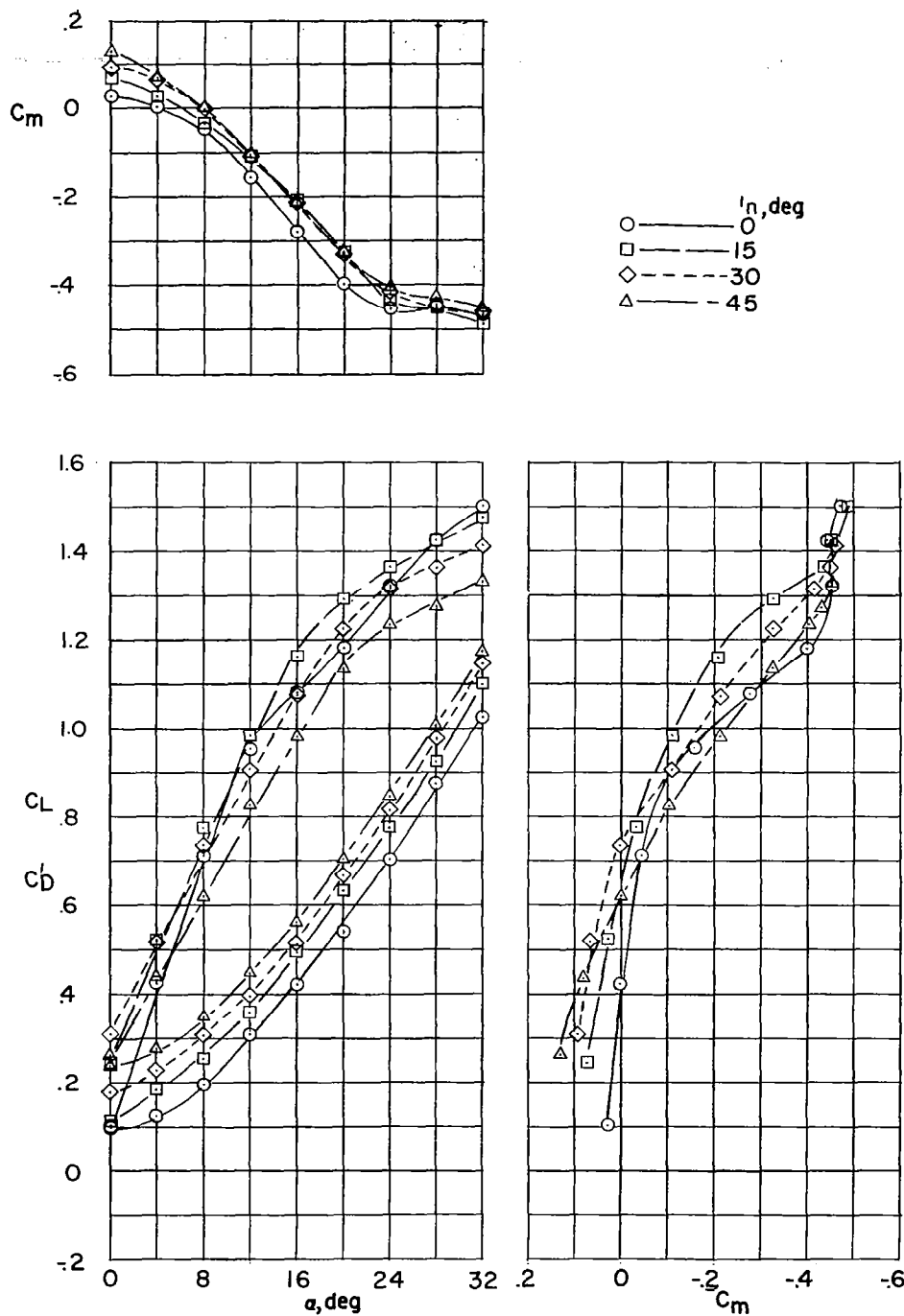


Figure 9.- Effect of nacelle incidence on longitudinal stability characteristics. Nacelle inlets retracted.

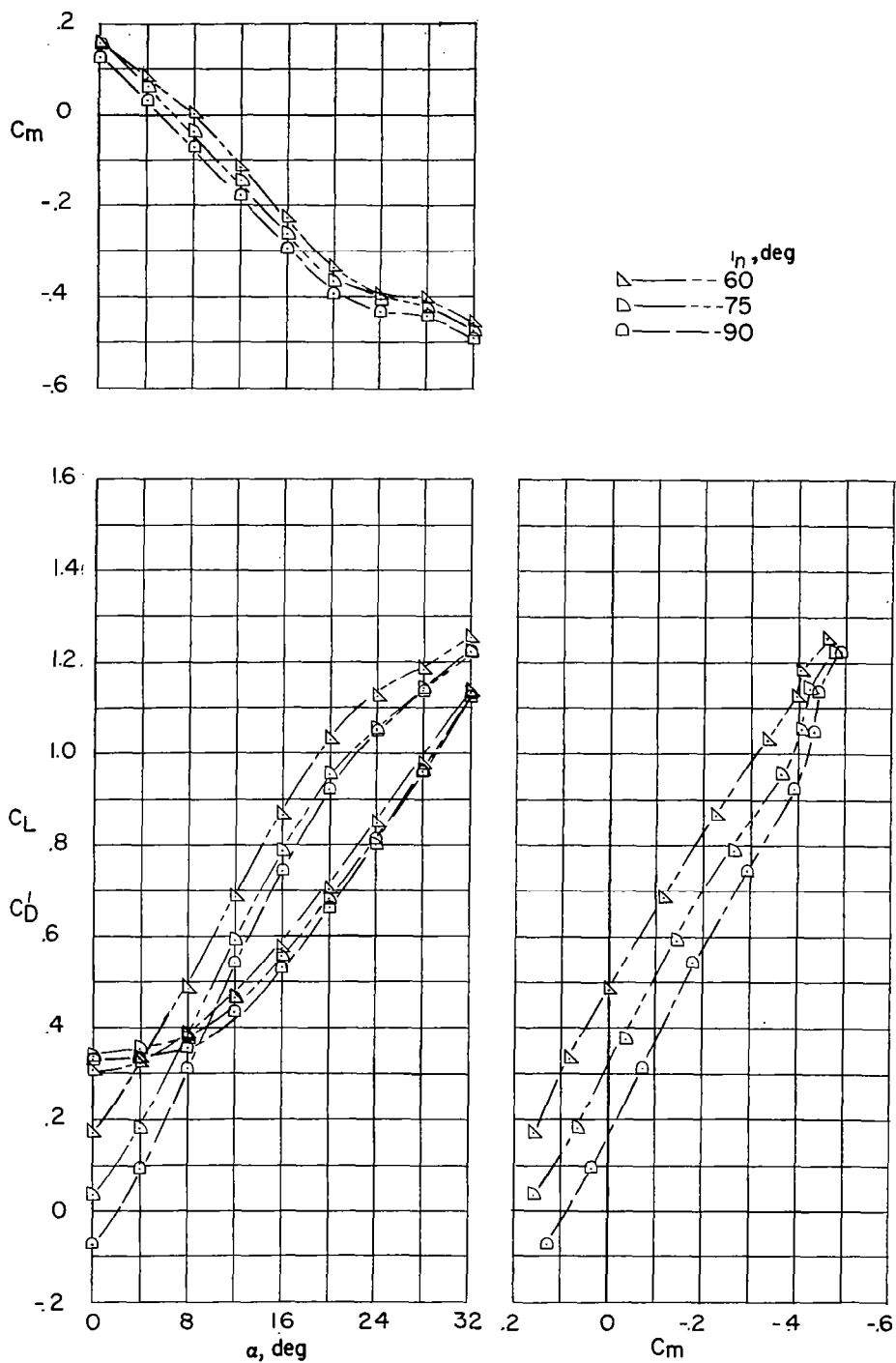
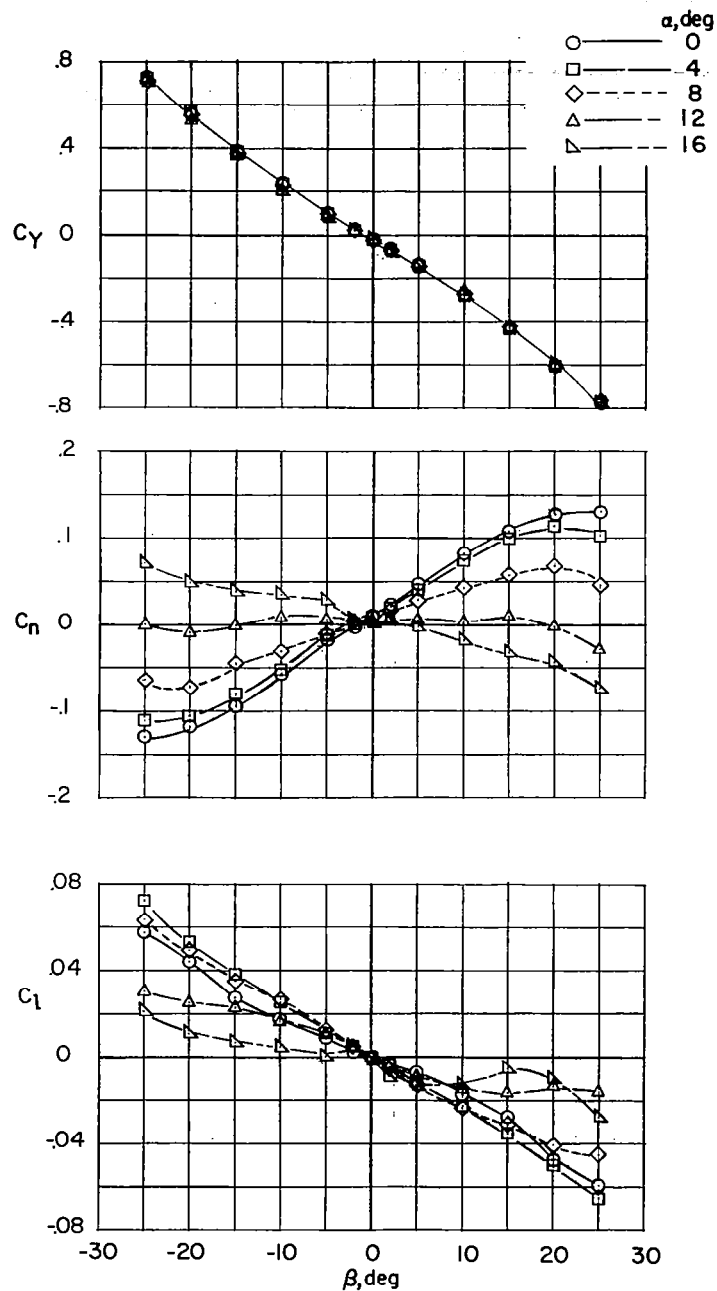
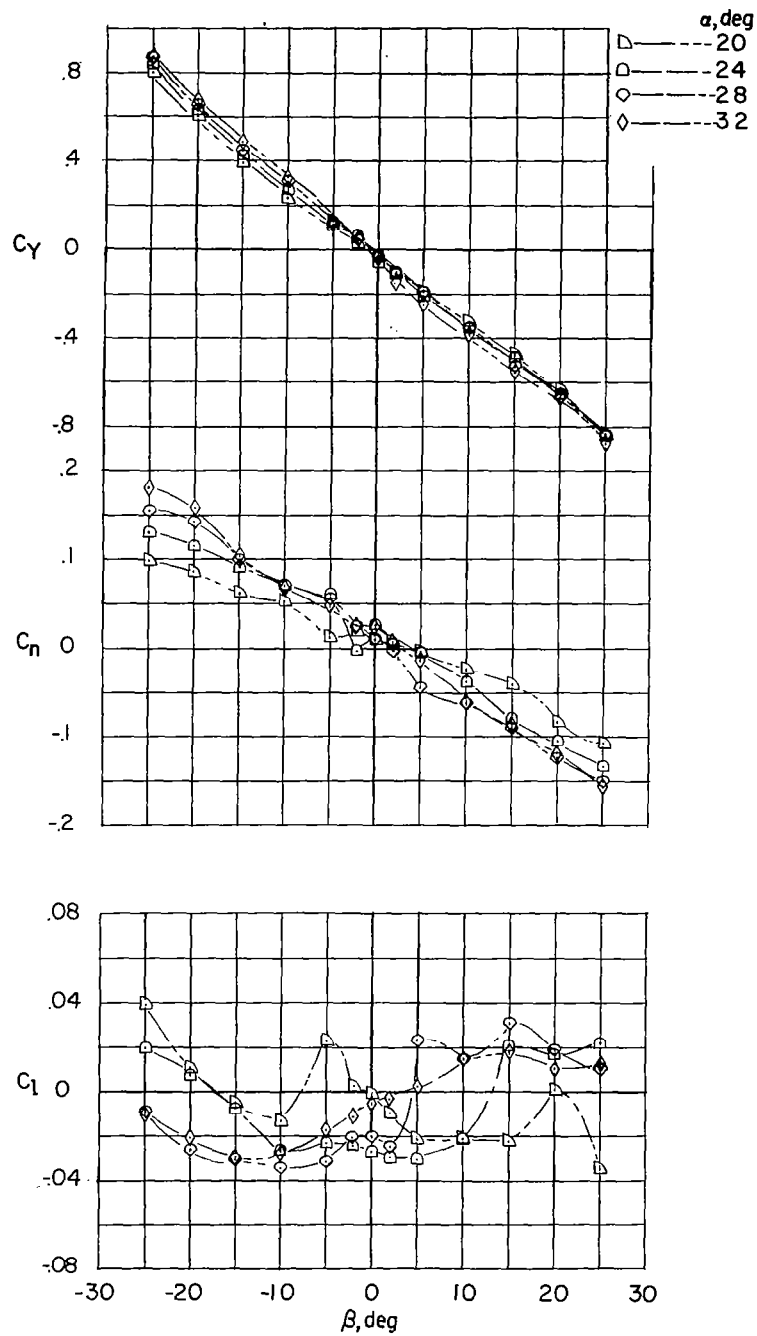


Figure 9.- Concluded.



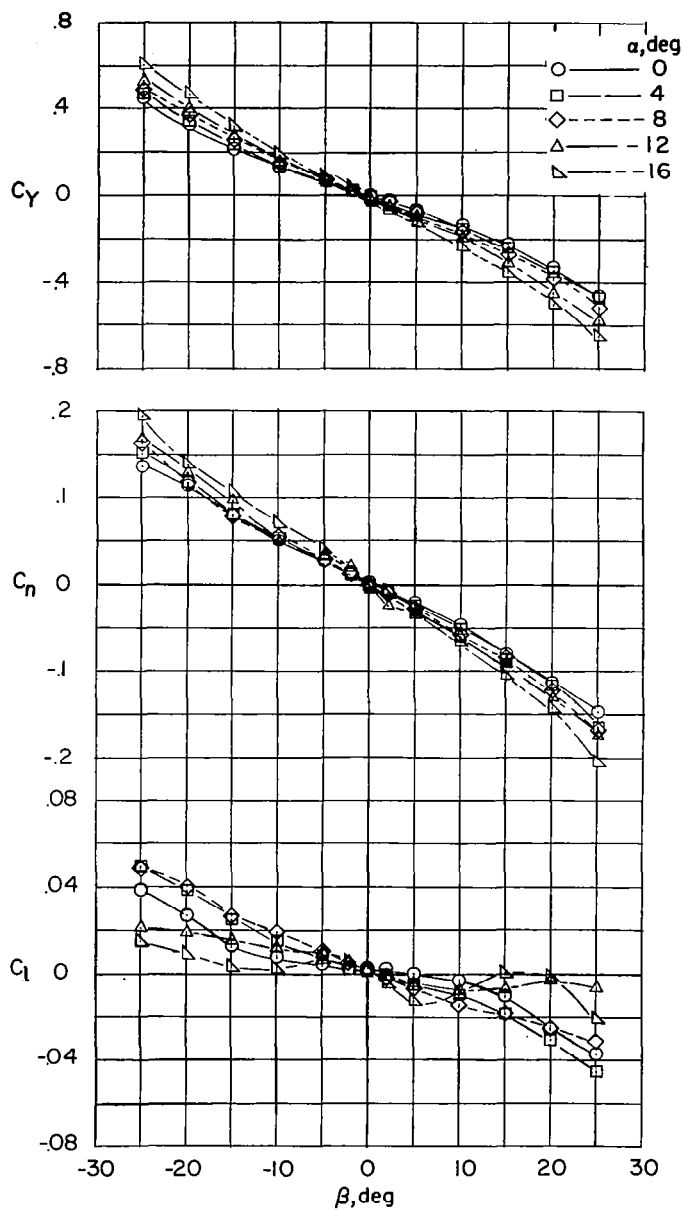
(a) Vertical tails on.

Figure 10.- Lateral stability characteristics of model with nacelle inlets in retracted position. $i_n = 0^\circ$.



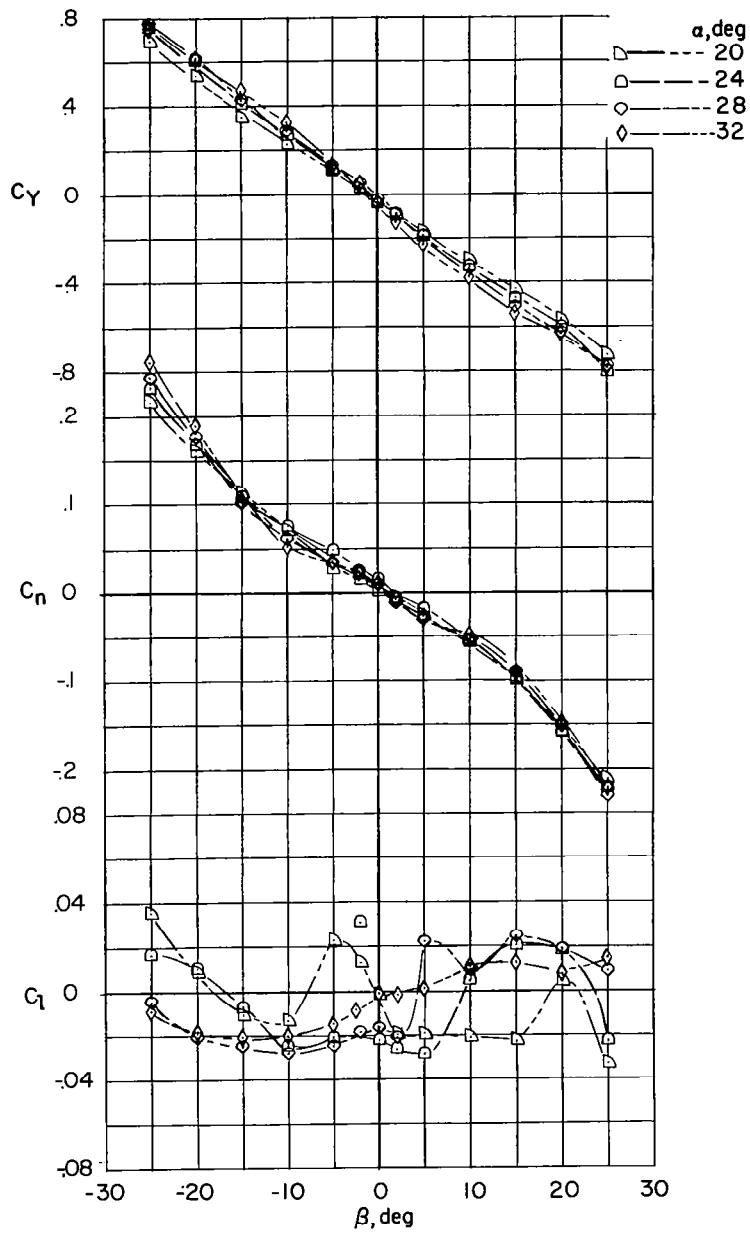
(a) Concluded.

Figure 10.- Continued.



(b) Vertical tails off.

Figure 10.- Continued.



(b) Concluded.

Figure 10.- Concluded.

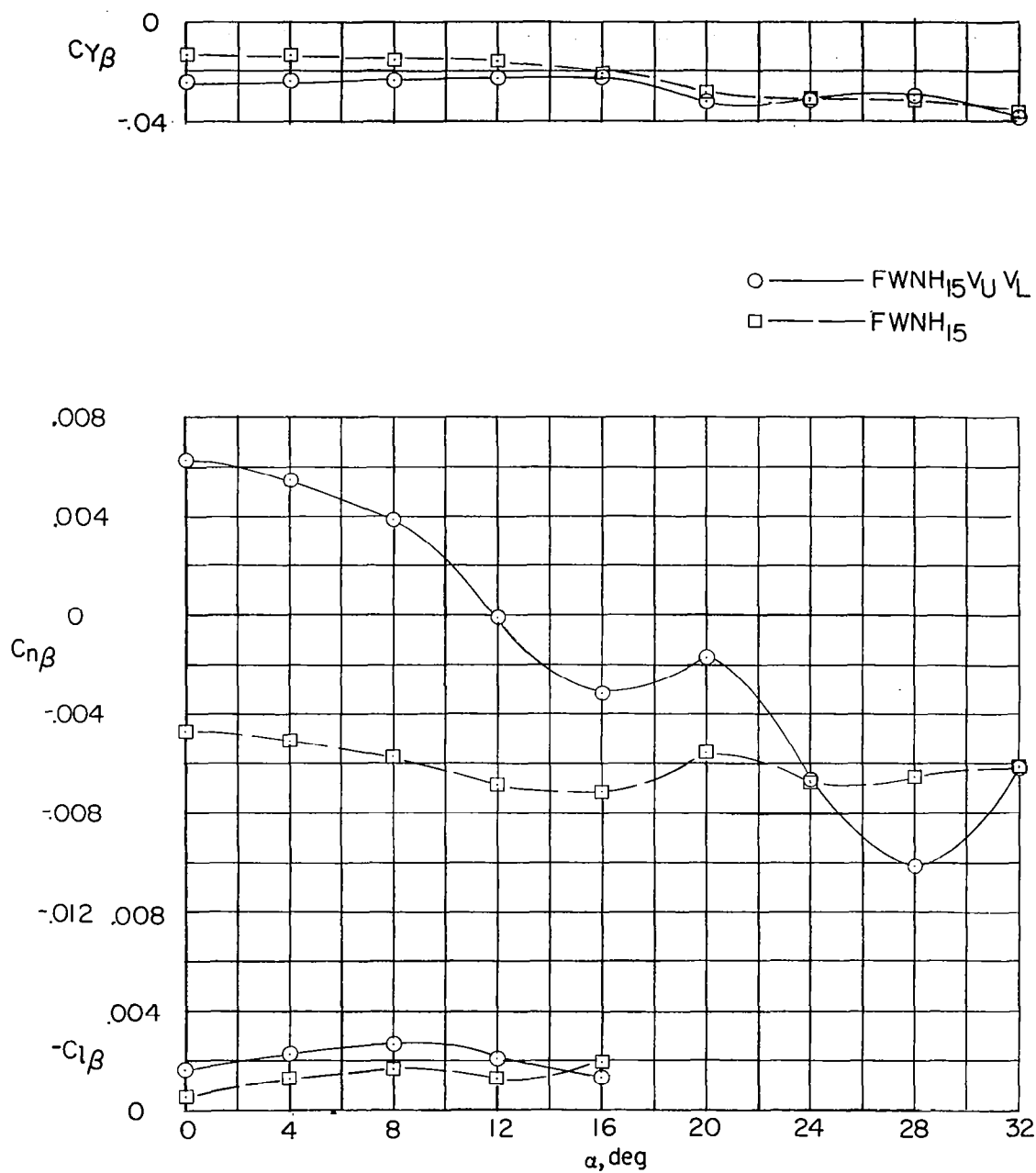


Figure 11.- Variation of lateral stability derivatives with angle of attack. Inlet retracted; $i_n = 0^\circ$.

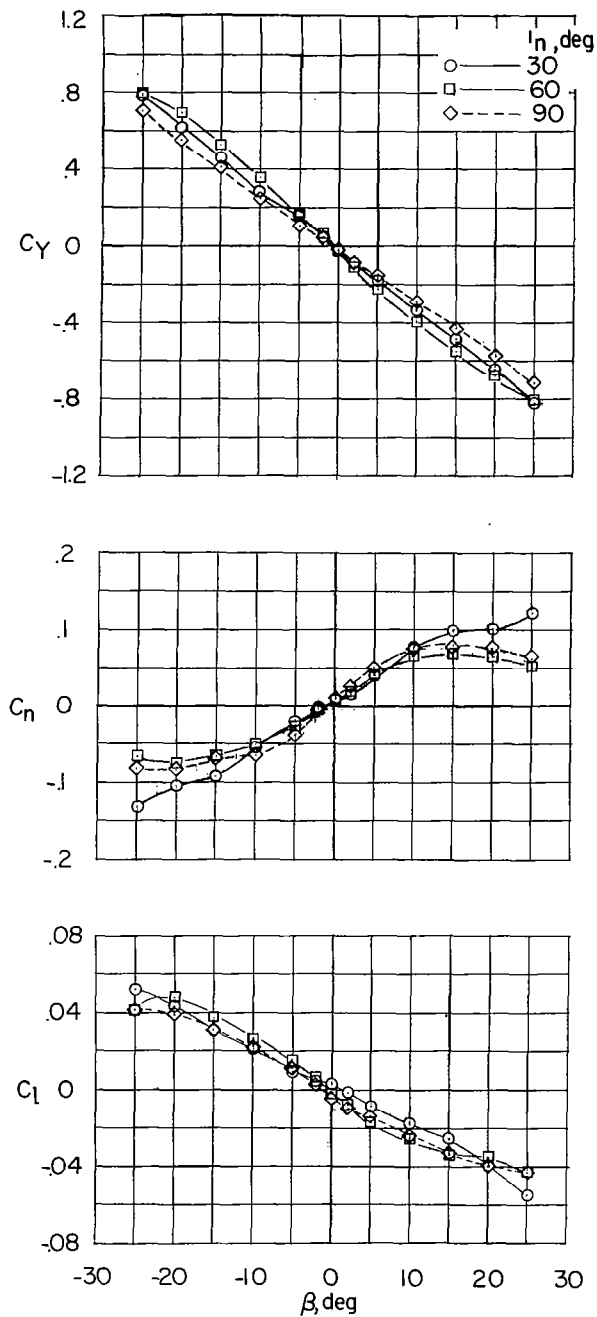
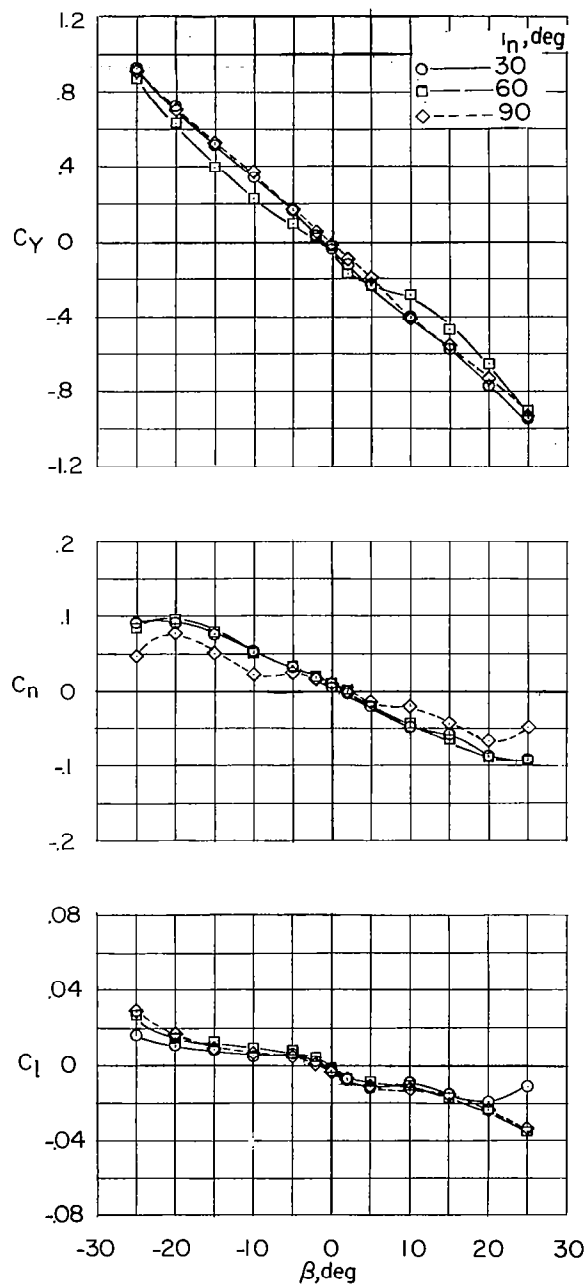
(a) $\alpha = 0^\circ$.

Figure 12.- Effect of nacelle incidence on lateral stability characteristics. Inlets retracted.



(b) $\alpha = 20^\circ$.

Figure 12.- Concluded.

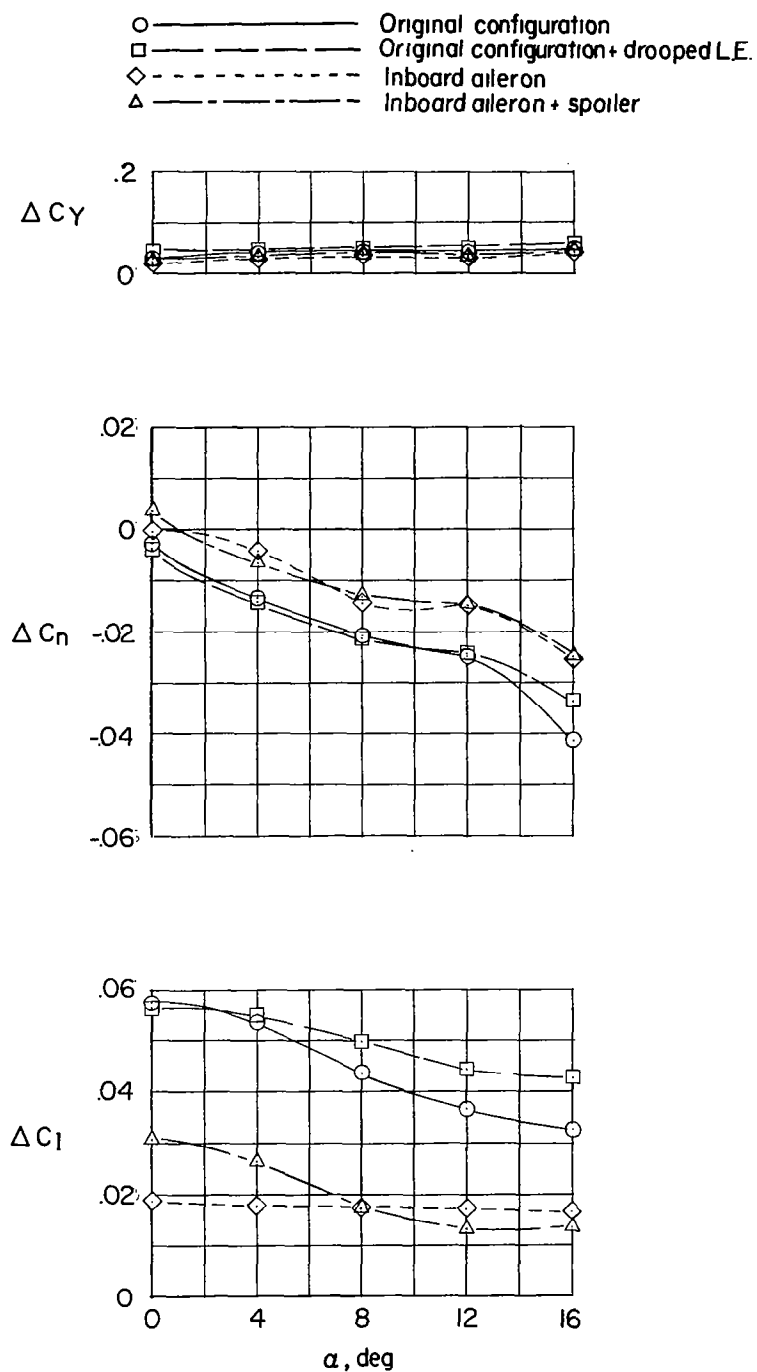
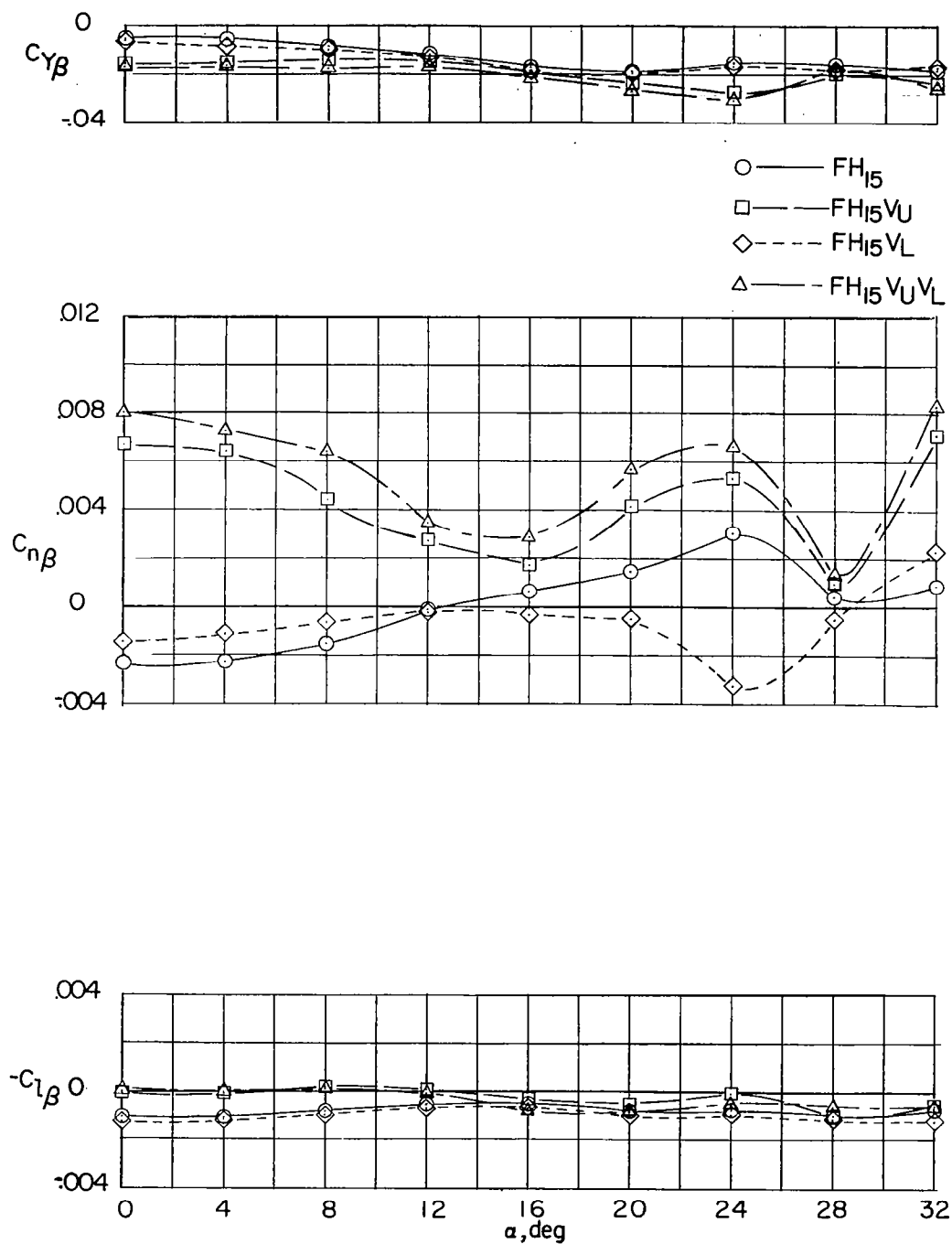
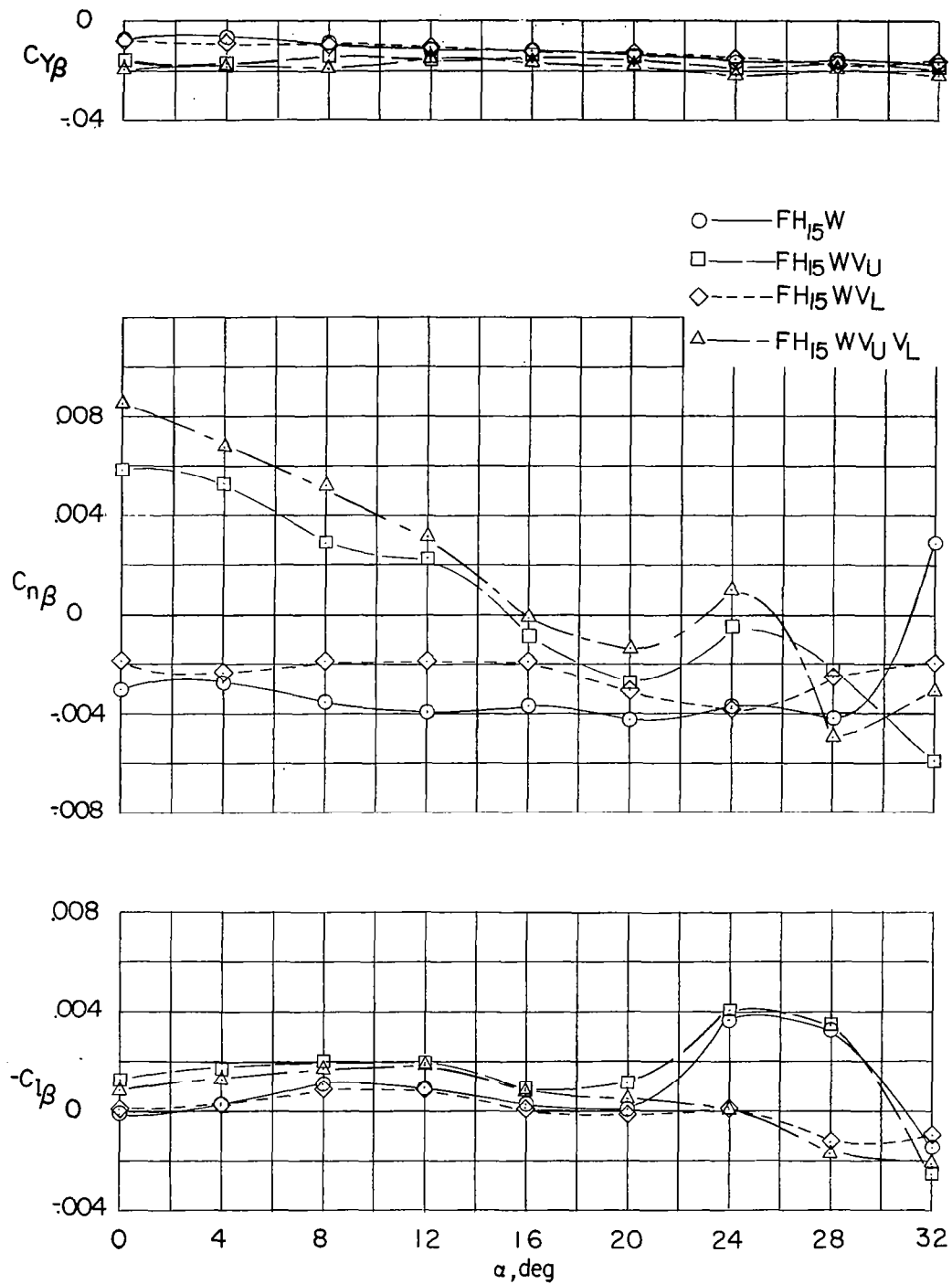


Figure 13.- Aileron effectiveness. Configuration FWNH₁₅V_UV_L with nacelle inlets extended; $i_n = 0^\circ$; $\delta_{a_l} = 20^\circ$; $\delta_{a_r} = -20^\circ$.



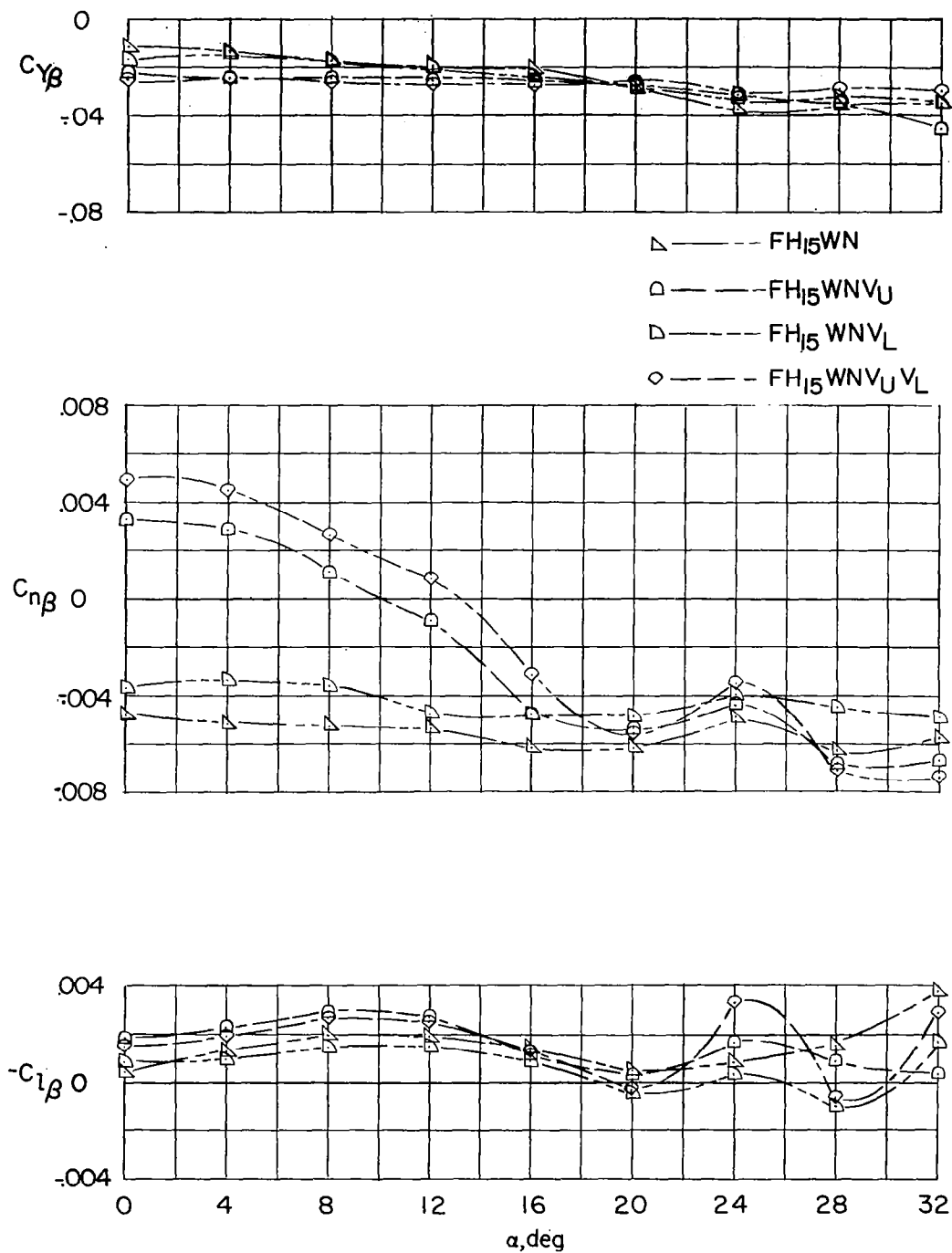
(a) Wing and nacelles off.

Figure 14.- Effect of various components on lateral stability derivatives.



(b) Wing on, nacelles off.

Figure 14.- Continued.



(c) Wing and nacelles on. Inlets extended; $i_n = 0^\circ$.

Figure 14.- Concluded.

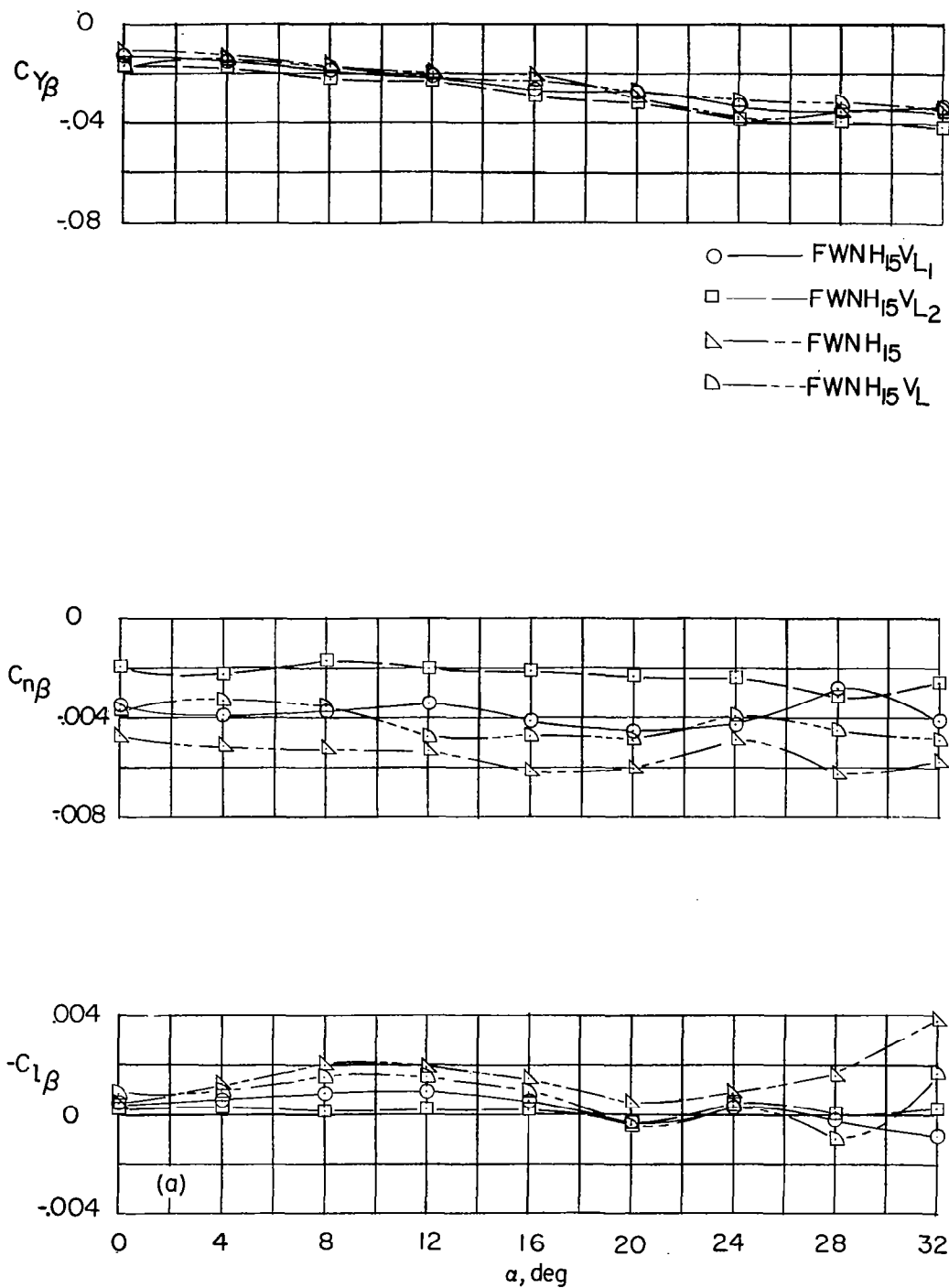


Figure 15.- Effect of lower vertical-tail modifications on lateral stability derivatives. Inlets extended; $i_n = 0^\circ$.

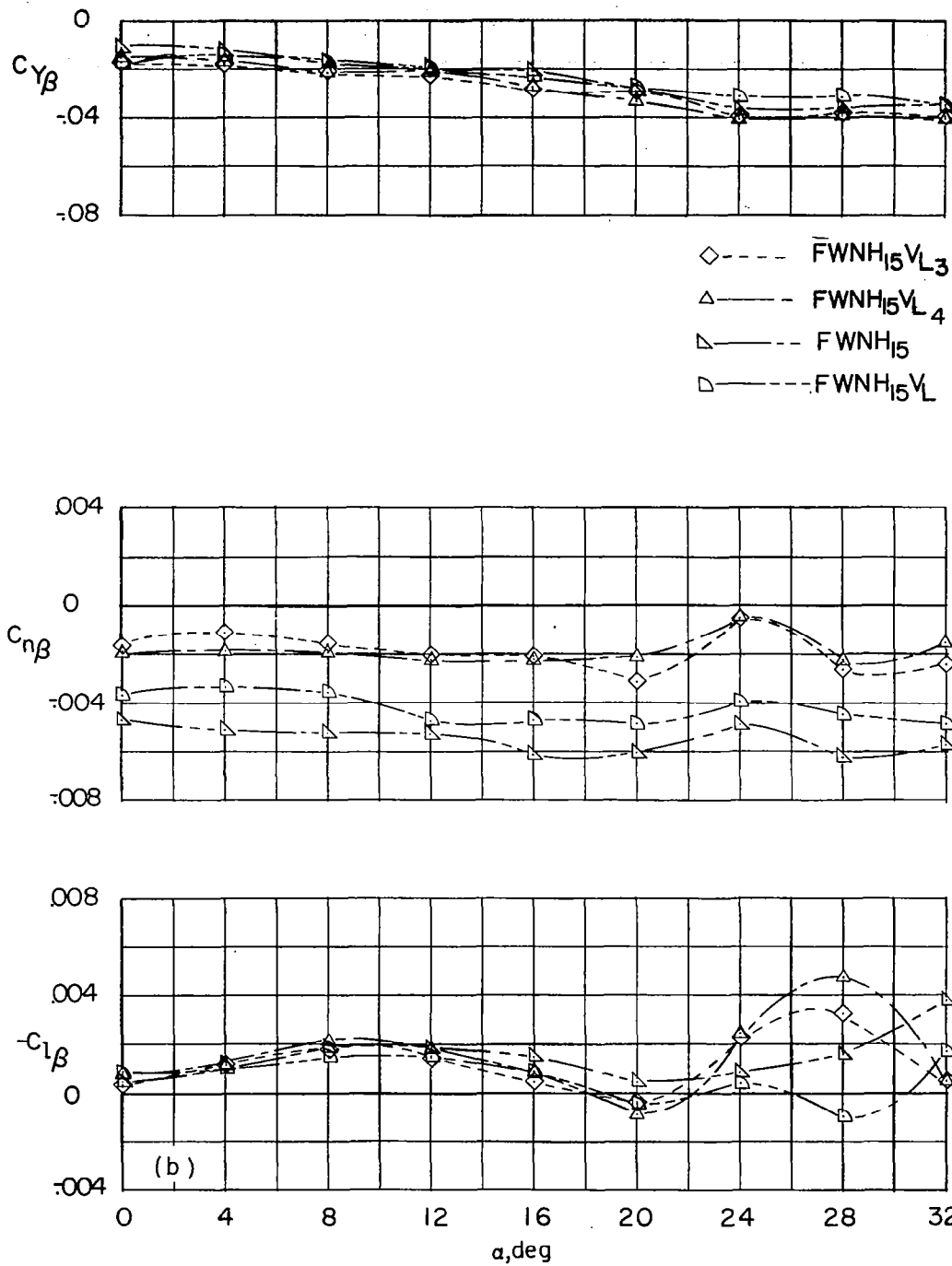


Figure 15.- Concluded.

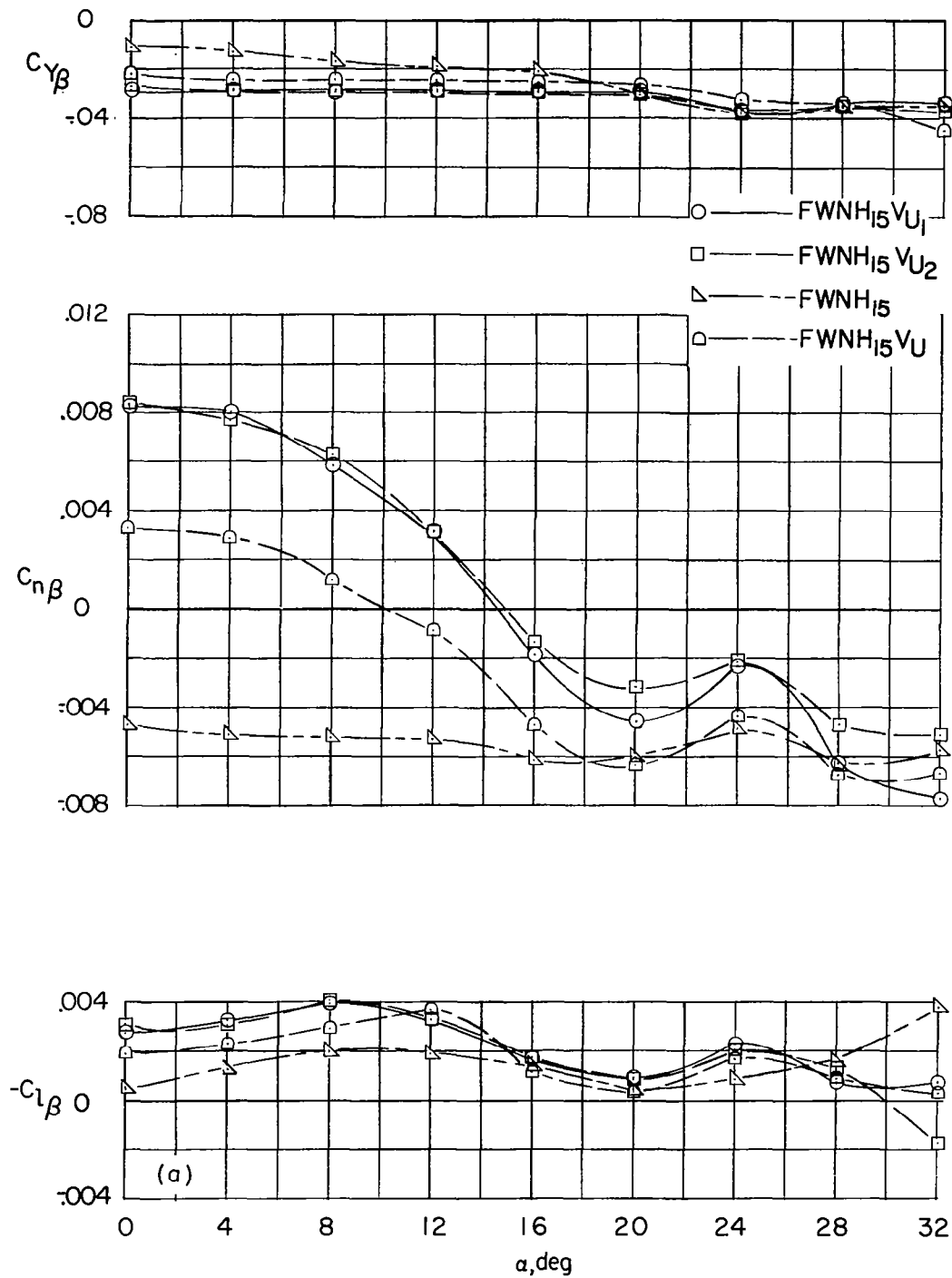


Figure 16.- Effect of upper vertical-tail modifications on lateral stability derivatives. Inlets extended; $i_n = 0^\circ$.

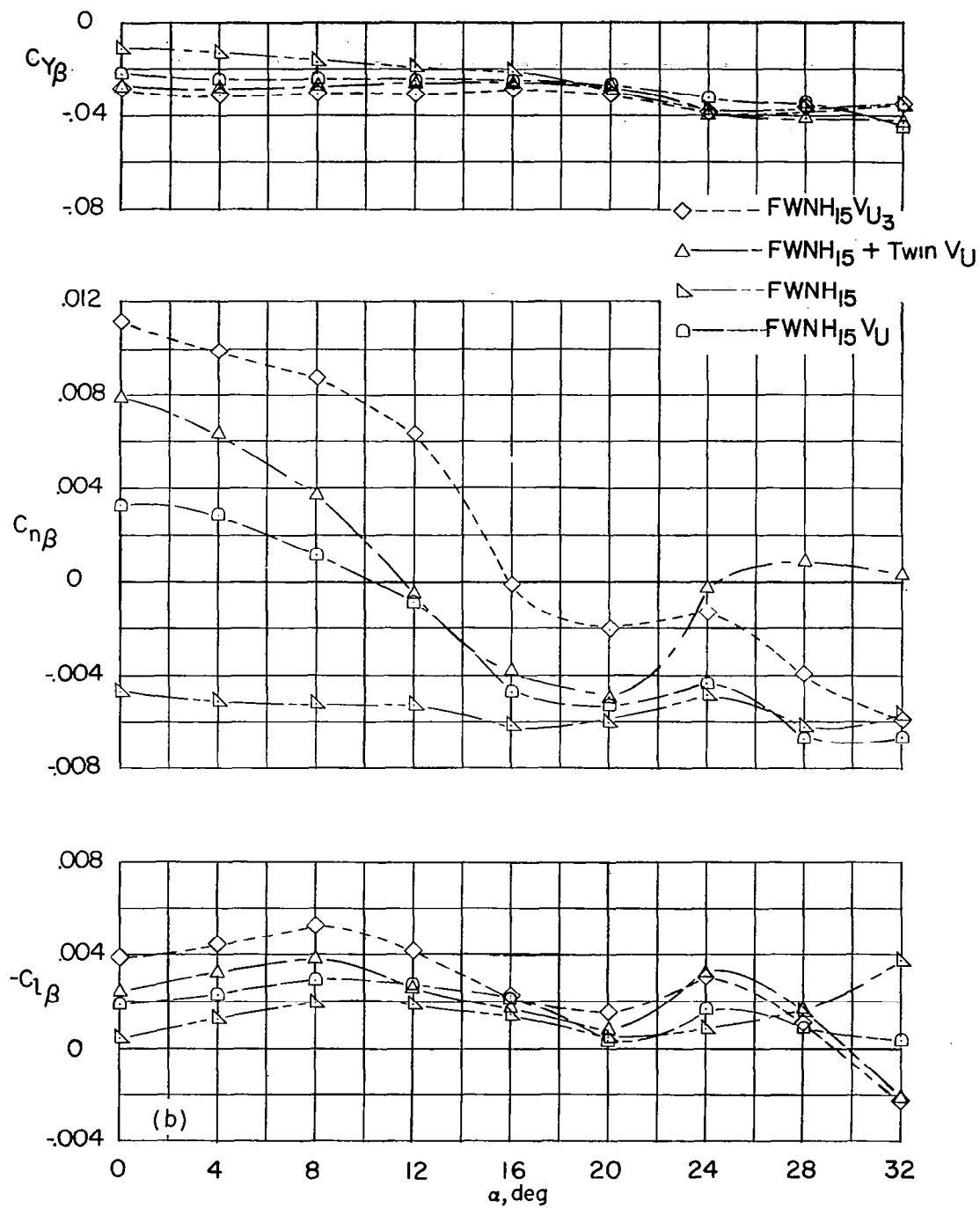


Figure 16.- Concluded.

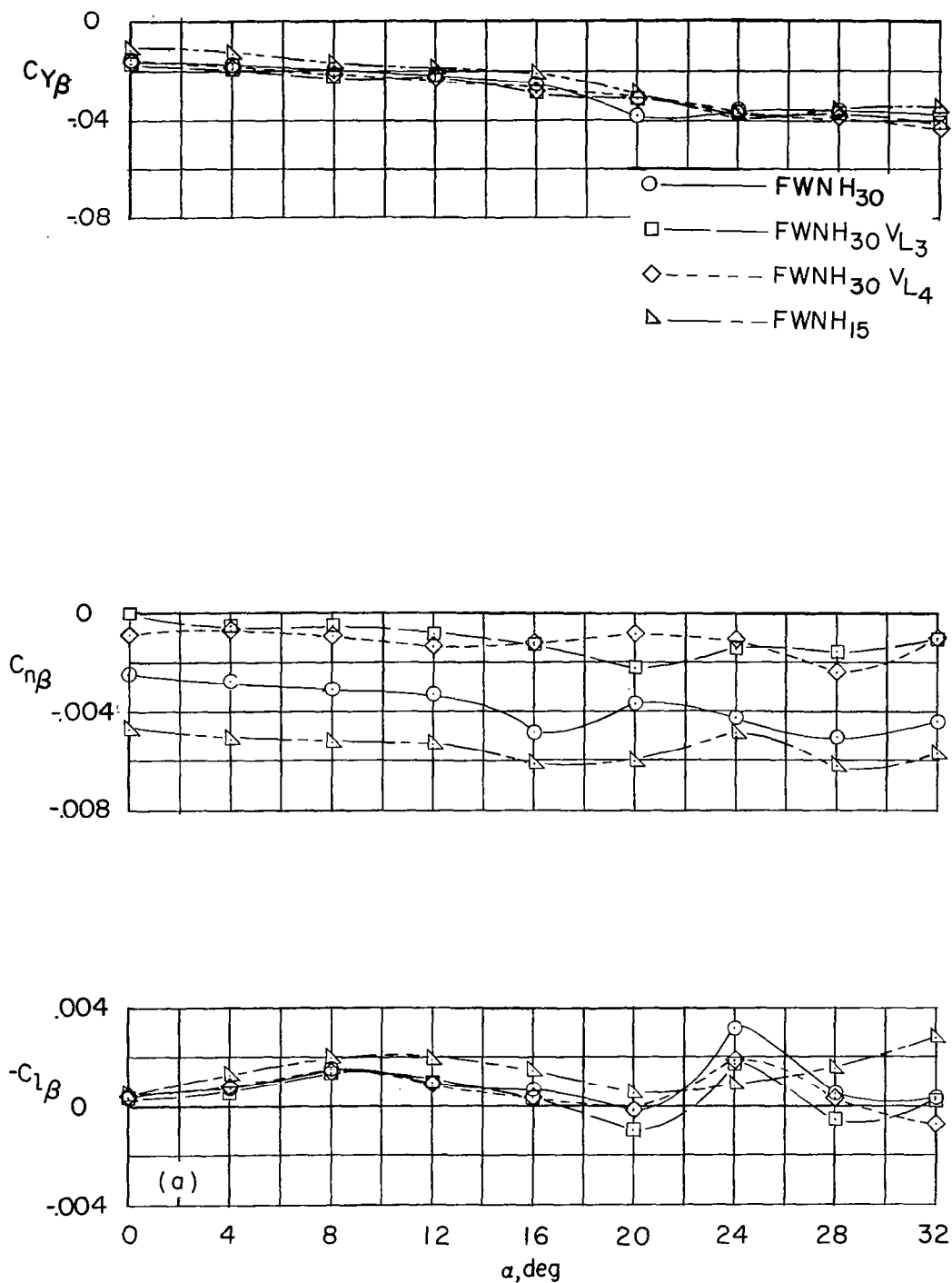


Figure 17.- Effect of horizontal tail dihedral on lateral stability derivatives. Inlets extended; $i_n = 0^\circ$.

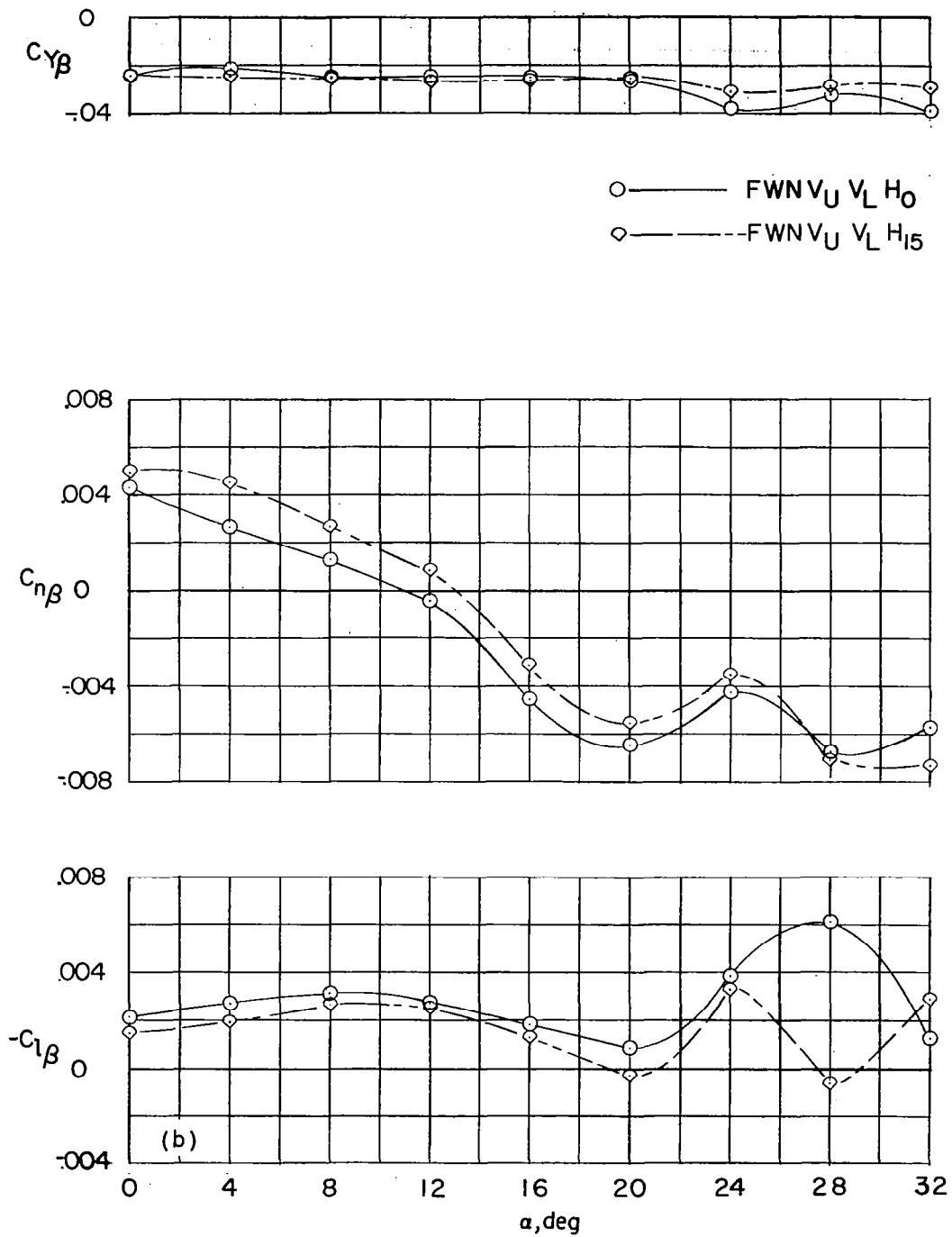


Figure 17.- Concluded.

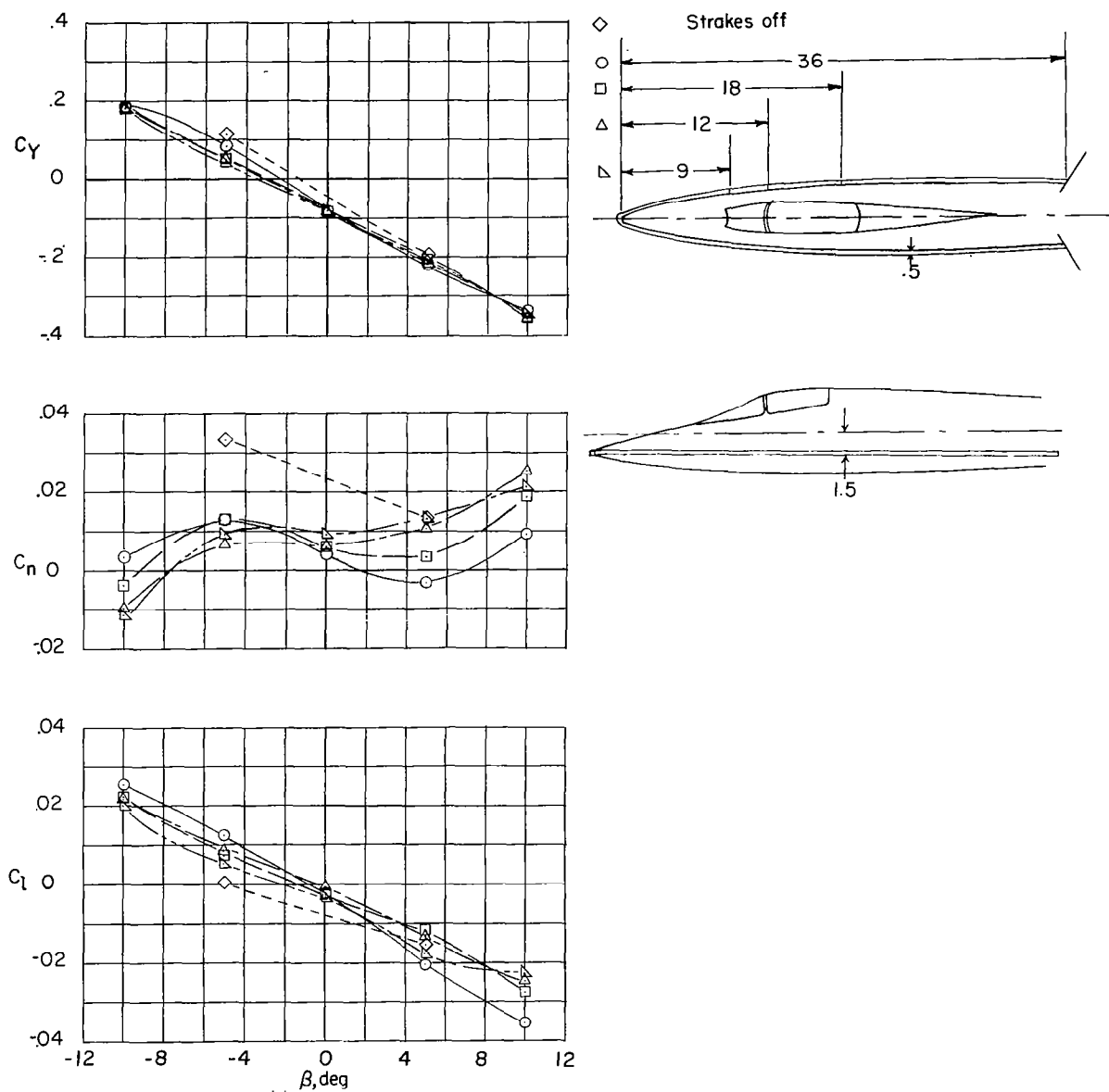
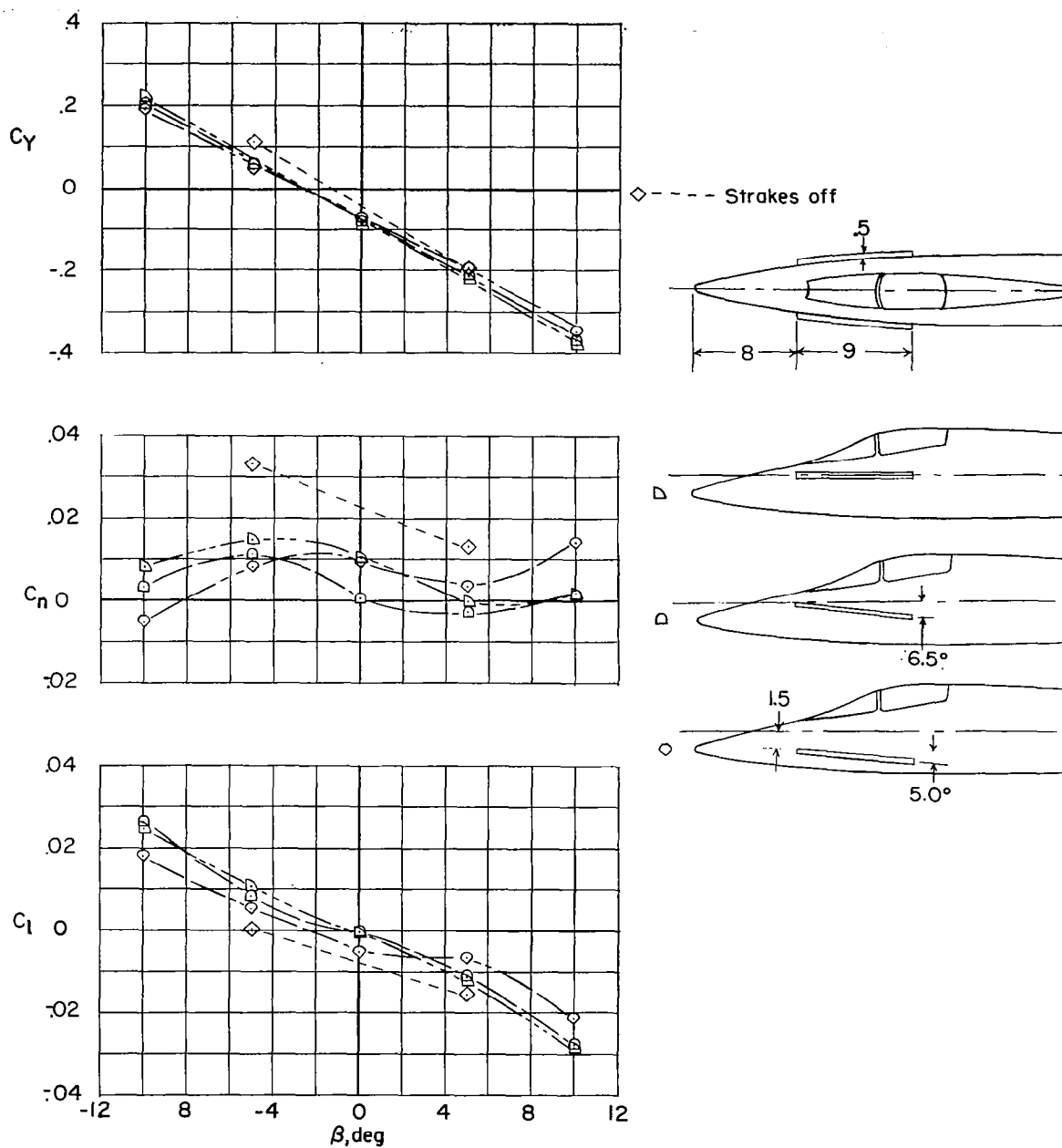
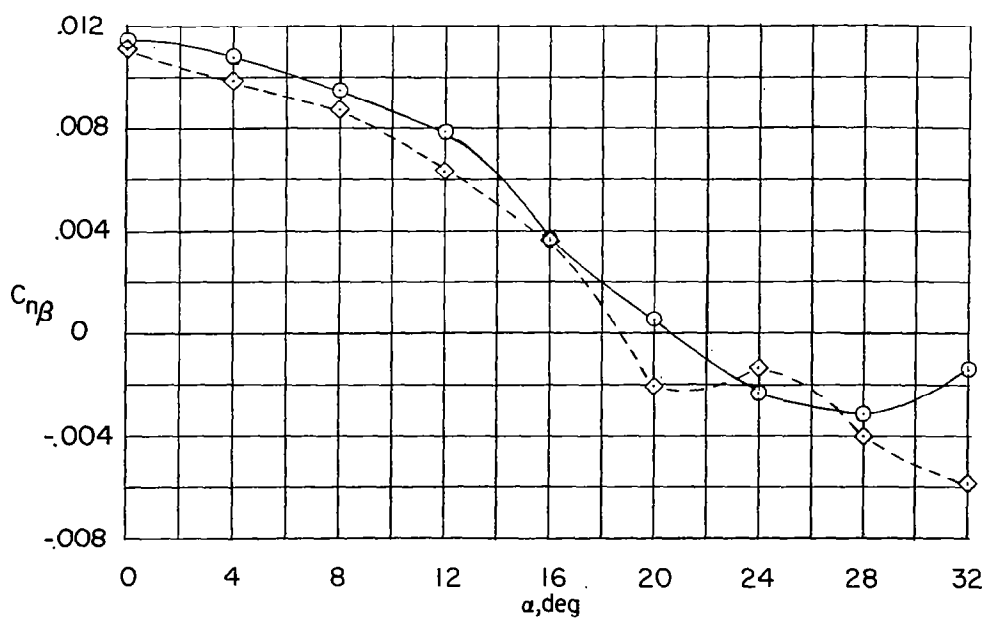
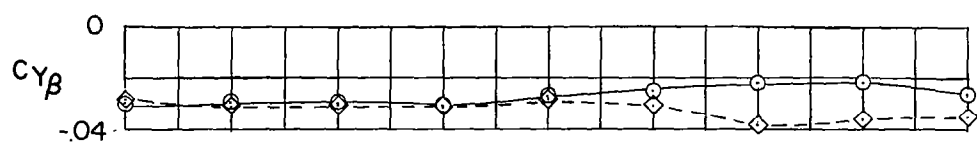
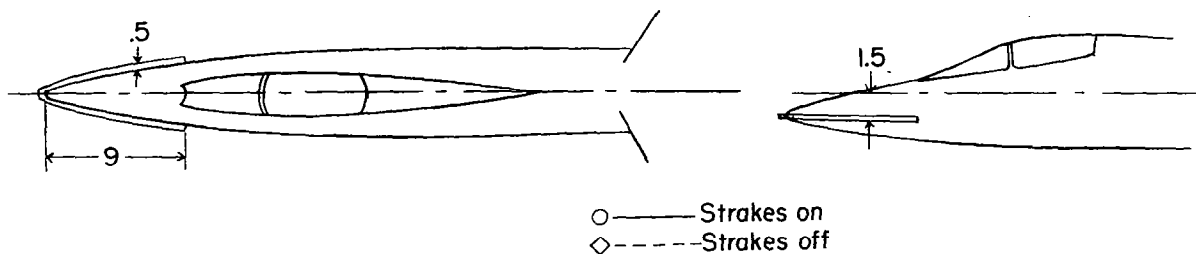
(a) $\alpha = 20^\circ$.

Figure 18.- Effect of strakes on lateral stability characteristics. Configuration FWNH₁₅VU₃ with nacelle inlets extended. All dimensions are in inches.



(a) Concluded.

Figure 18.- Continued.



(b) Variation of lateral stability derivatives with α .

Figure 18.- Concluded.

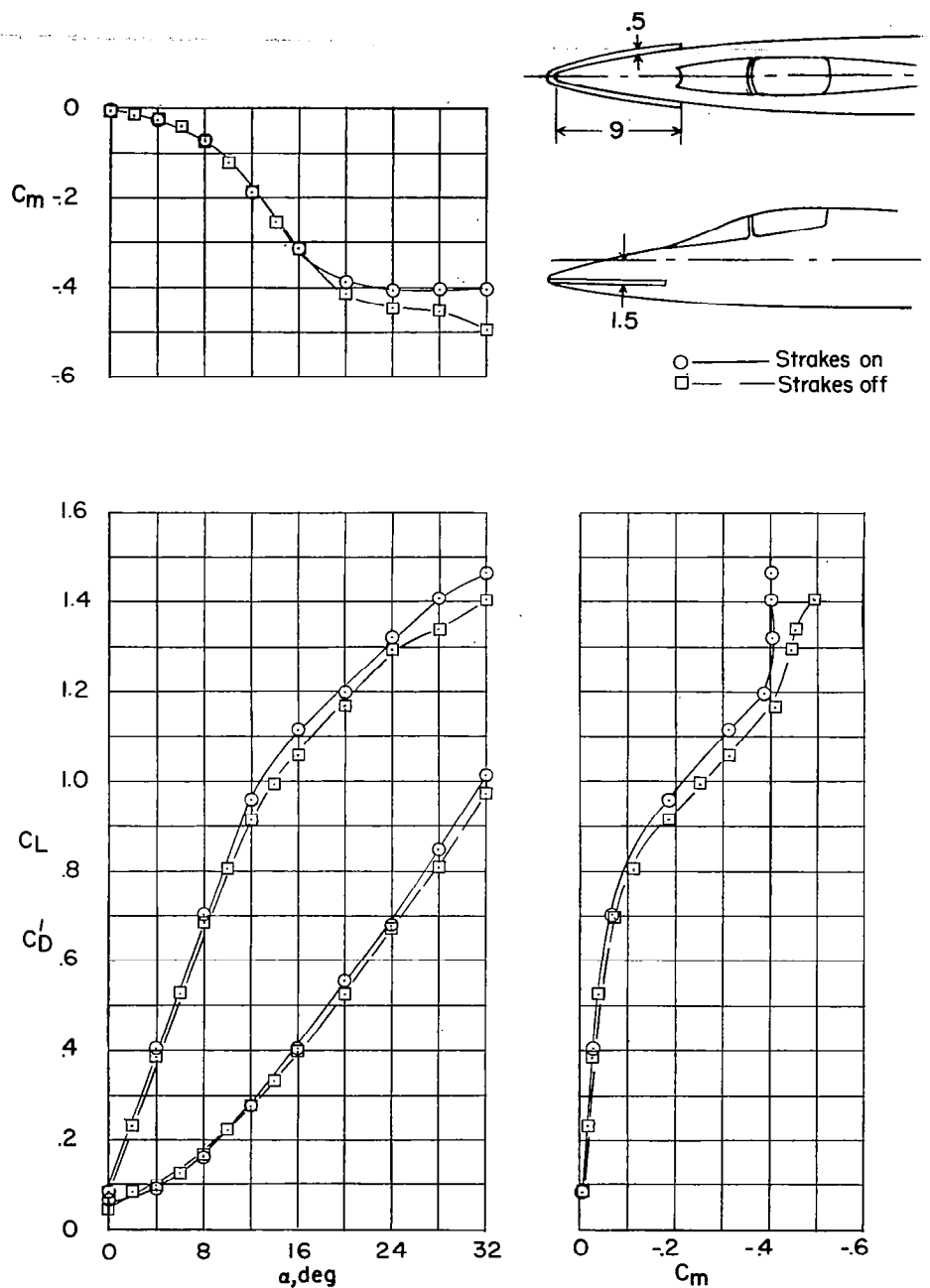


Figure 19.- Effect of strakes on longitudinal stability characteristics. Configuration FWNH₁₅VU₃ with nacelle inlets extended; $i_n = 0^\circ$. All dimensions are in inches.

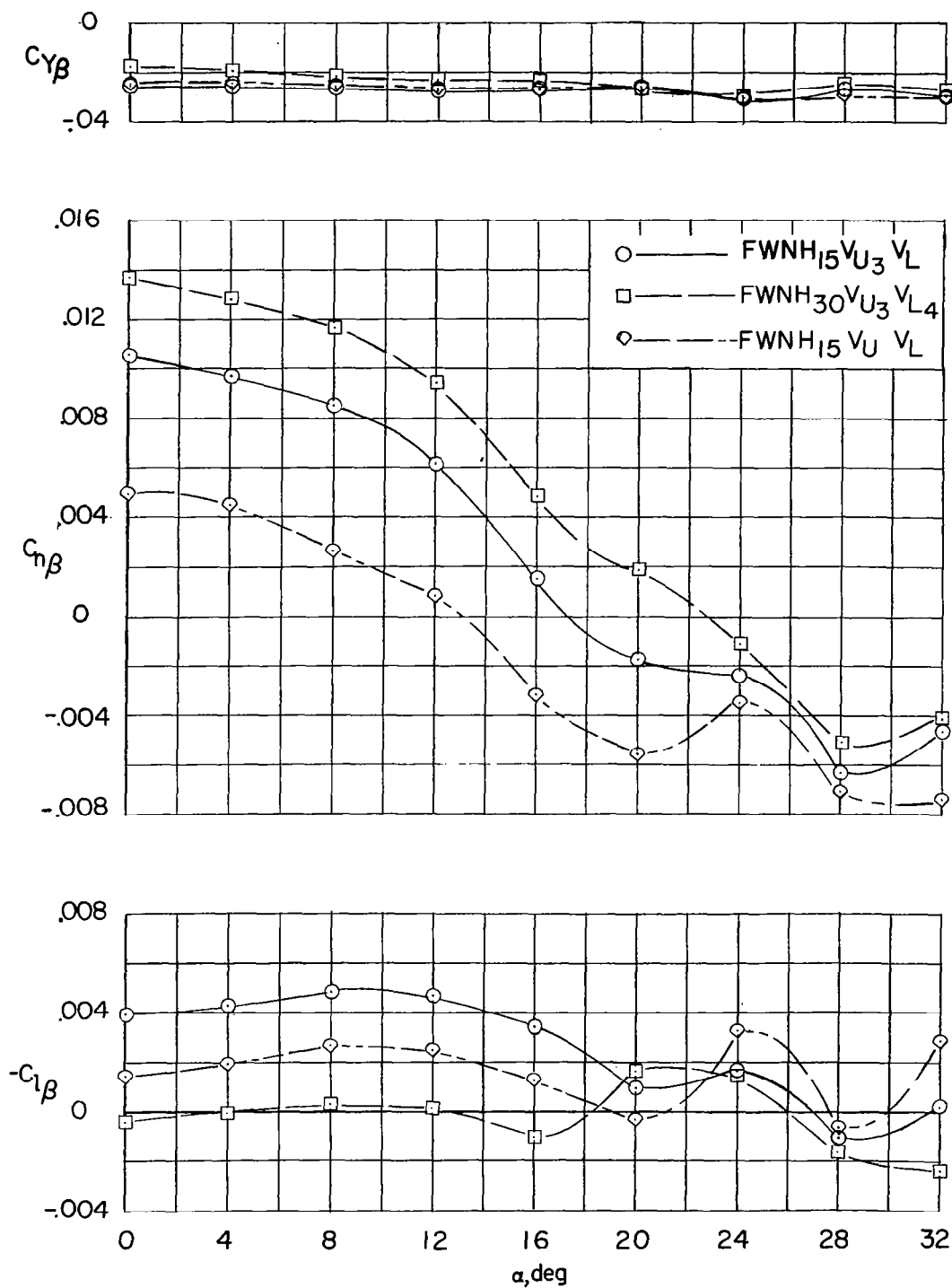


Figure 20.- Effect of combinations of modified vertical tails on lateral stability derivatives. Inlets extended; $i_n = 0^\circ$.

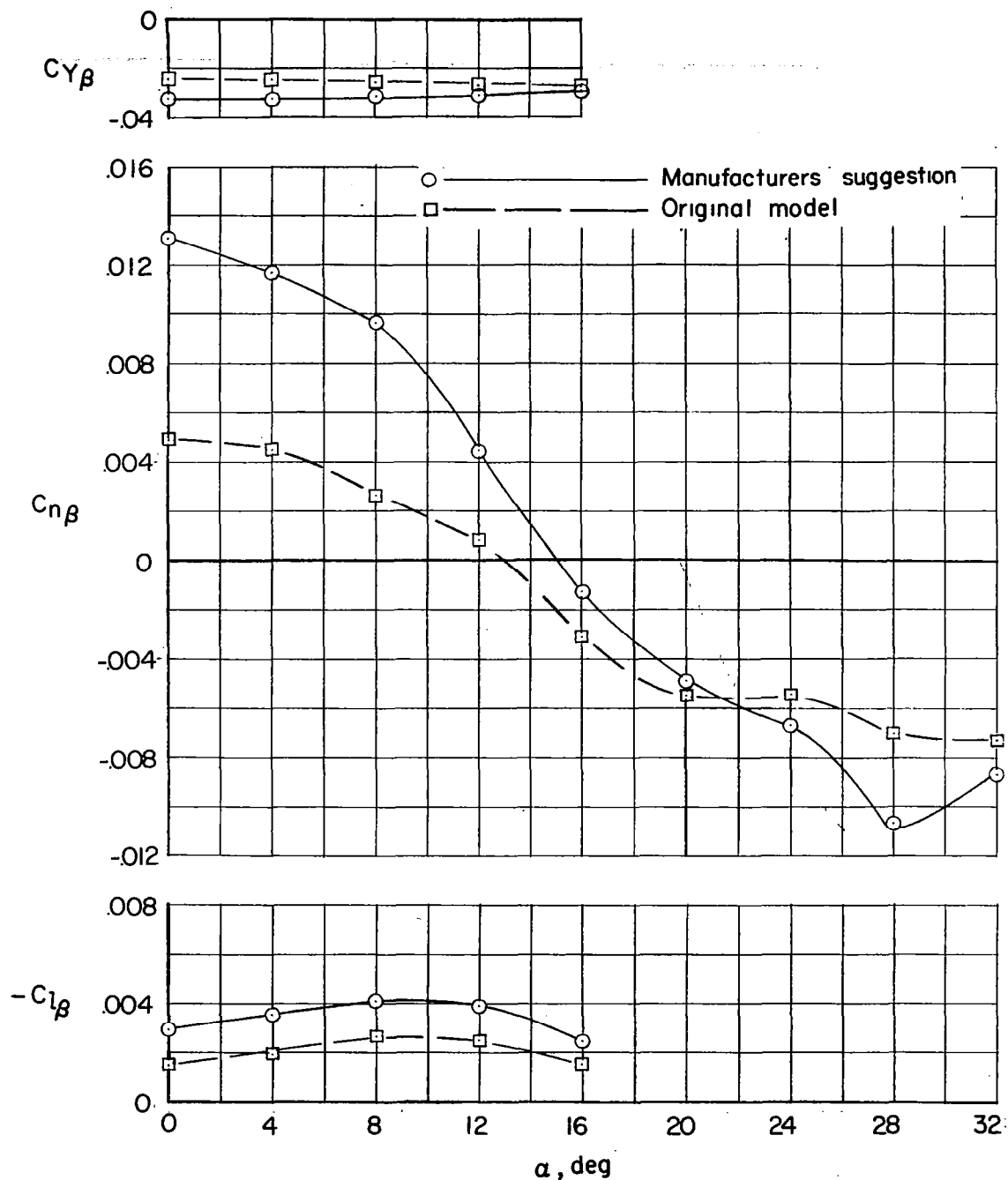


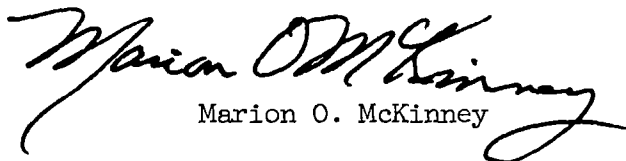
Figure 21.- Effect of the vertical-tail arrangement suggested by the manufacturer on lateral stability derivatives. Inlet extended; $i_n = 0^\circ$.


~~CONFIDENTIAL~~


NACA RM SL58H15

LOW-SPEED WIND-TUNNEL TESTS OF A 1/8-SCALE
MODEL OF THE BELL D-188A VTOL AIRPLANE

TED NO. NACA AD 3147


Marion O. McKinney


Charles C. Smith, Jr.

Approved: 
Thomas A. Harris
Chief of Stability Research Division
Langley Aeronautical Laboratory

(8/1/58)
DY

~~CONFIDENTIAL~~

LOW-SPEED WIND-TUNNEL TESTS OF A 1/8-SCALE
MODEL OF THE BELL D-188A VTOL AIRPLANE*

TRD NO. NACA AD 3147

By Marion O. McKinney and Charles C. Smith, Jr.

ABSTRACT

The Bell D-188A VTOL airplane is a horizontal-attitude VTOL fighter with tilting engine nacelles at the tips of a low-aspect-ratio unswept wing. The static stability and control characteristics of the model were generally satisfactory except that the model was directionally unstable at angles of attack above 13° and that the aileron effectiveness dropped off markedly as the angle of attack was increased from 0° to 16° .

INDEX HEADINGS

Stability, Longitudinal - Static	1.8.1.1.1
Stability, Lateral - Static	1.8.1.1.2
Stability, Directional - Static	1.8.1.1.3
Control, Longitudinal	1.8.2.1
Control, Lateral	1.8.2.2

*Title, Confidential.

NASA Technical Library
3 1176 01438 9895